

Resonance radiation plasma (photoresonance plasma)

I. M. Beterov, A. V. Eletskiĭ, and B. M. Smirnov

Usp. Fiz. Nauk **155**, 265–298 (June 1988)

A plasma formed by the action on a gas of monochromatic radiation whose frequency corresponds to the energy of a resonance transition in the atom is studied. The elementary methods of creating and studying a plasma of this type are analyzed. The kinetics of formation of a photoresonance plasma is studied, including collision processes with participation of excited atoms leading to formation of molecular ions and highly excited atoms, processes of stepwise ionization and triple recombination, and radiative processes. A photoresonance plasma is characterized by a high electron density with a relatively low electron temperature; for this reason the condition of ideality is more easily violated in a plasma of this type. Some ways of utilizing a photoresonance plasma are presented.

TABLE OF CONTENTS

| | |
|---|-----|
| 1. Introduction | 535 |
| 2. Types of photoresonance plasmas and methods of preparing them | 536 |
| 2.1. Photoresonance non-laser plasmas. 2.2. Photoresonance laser plasmas. | |
| 2.3. Quasiresonance plasmas. 2.4. Beam and jet photoresonance plasmas. | |
| 3. Elementary processes in a photoresonance plasma | 541 |
| 3.1. Photoprocesses. 3.2. Collision of electrons with excited atoms. 3.3. Ionization with participation of excited atoms. | |
| 4. Properties of photoresonance plasmas | 545 |
| 4.1. Establishment of equilibrium in photoresonance plasmas. 4.2. Nonideal photoresonance plasmas. | |
| 5. Optogalvanic spectroscopy | 551 |
| 5.1. The optogalvanic effect. 5.2. Laser isotope analysis. | |
| 6. Conclusion | 552 |
| References | 553 |

1. INTRODUCTION

One of the methods of creating a plasma involves the action of optical resonance radiation on a gas. This method was first realized by Mohler and Boeckner,¹ who observed the formation of ions upon irradiating cesium vapor with resonance radiation. Thus they established the possible occurrence in the gas of the process of associative ionization, in which an electron and a molecular ion are formed by collision of excited and unexcited atoms, so that the energy needed for ionizing the atom is released through formation of a molecular ion. Studies of photoresonance plasmas (PRPs) began with the study of Morgulis, Korchevoi, and Przhonskii² in 1967. By illuminating cesium vapor with resonance radiation to obtain a gas with a high concentration of excited atoms, they found as a result that a plasma is formed with a rather high concentration of charged particles. Since the ionization energy of the cesium atom (3.89 eV) exceeds by more than twofold the energy of a resonance photon (1.39 or 1.45 eV), this result indicated a complex, multistep character of the kinetics of the ionization of cesium atoms under the conditions studied. The subsequent detailed studies of this kinetics^{3–5} have permitted obtaining rich information on the mechanisms and rates of processes involving excited atoms.

The formation of a photoresonance plasma is accompanied by various phenomena that occur in gases. Thus, the ionization of a gas under the action of resonance optical radiation is one of the fundamental mechanisms of formation of an ionization wave in the gas, which propagates upon apply-

ing an external electric field.⁶ This same mechanism plays the decisive role in the phenomenon of ionization of a gas ahead of the front of a strong shock wave in the gas.⁷ Irradiation of a gas with optical resonance radiation is used as one of the methods of preliminary ionization of the active medium of high-pressure molecular lasers.³ This enables one to create a plasma homogeneous throughout the volume, while avoiding the factors that favor the development of instabilities and spatial inhomogeneities of the active medium.³ The stated method of creating a high-density plasma homogeneous throughout the volume has attracted the attention of investigators also in connection with the problem of heating thermonuclear targets with beams of light ions.⁸ In this case the ionization of the gas under the action of resonance radiation enables one to create for a short time an extended plasma channel, which serves for transport of the ion beam to the target, while hindering electrostatic repulsion of the ions.⁹

The potentialities of study of photoresonance plasmas, as well as the set of their applications, have been expanded by the invention of frequency-tunable lasers. On the one hand, this has enabled considerable increase in the fluxes of resonance radiation transmitted through the gas, and on the other hand, study of the processes that occur upon optical excitation of various states of the atom. The photoresonance plasma formed by using tunable lasers is used as a nonlinear element in frequency transformation of laser radiation,¹⁰ as a source of ions of a given type,^{11–13} etc.

The set of phenomena that occur in a photoresonance plasma is closely bordered by the optogalvanic effect, which

consists in a change in the electrical properties of a gas-discharge plasma or flame (e.g., the volt-ampere characteristics) when acted on by optical resonance radiation.¹⁴ The optogalvanic effect is used for determining trace impurities of elements in a gas, in studying the mechanisms of elementary processes in a gas-discharge plasma, in controlling the parameters of a gas-discharge plasma for transmission and processing of information, and as a detection method in laser spectroscopy with superhigh sensitivity.

The process of multistep ionization of atoms opens up broad possibilities. The use for this purpose simultaneously of several frequency-tunable lasers enables one to transfer an appreciable number of atoms of a certain type to a given highly excited state. This technique, usually based on using atomic beams, is applied for detecting individual atoms, for detecting submillimeter radiation, for generating coherent radiation in the UHF range (maser), and in experiments on laser isotope separation.¹⁵ The identification of highly excited atoms is performed by ionizing them in an external electric field. Here one uses the sharp dependence of the ionization probability in a field of given intensity on the effective value n^* of the principal quantum number of a highly excited atom. The ions formed by ionization are extracted from the system by applied fields.

The properties and specifics of a photoresonance plasma are associated with the processes that occur in them. Thus a photoresonance plasma whose properties are determined by elementary collision-radiation processes, is naturally distinguished from a laser plasma, in which the transformation of the energy of the laser radiation into the energy of plasma particles results from the excitation of collective motions in the plasma.

At the same time it seems natural to classify as a photoresonance plasma one formed by the action of a gas of radiation having a frequency that does not necessarily correspond to a resonance transition, but also to transitions between ground and highly excited states, or transitions between two excited states. In all objects of this type, the fundamental ionization mechanism is collisional processes involving excited atoms (more rarely—molecules).

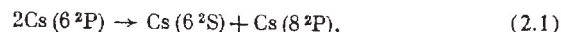
This review will analyze the current status of studies of photoresonance plasmas, information will be presented on the properties and parameters of this object, and problems will be discussed involving the application of photoresonance plasmas in the technique of physical experimentation and in applied fields.

2. TYPES OF PHOTORESONANCE PLASMAS AND METHODS OF PREPARING THEM

2.1. Photoresonance non-laser plasmas

The most convenient method of obtaining a photoresonance plasma not involving the use of laser radiation consists in irradiating a gaseous substance with a gas-discharge lamp filled with the same substance. Here the parameters of the photoresonance plasma are determined by the intensity of the resonance radiation emitted by the lamp. The most interesting results have been obtained in cases in which the lamp is characterized by a high coefficient of transformation of electrical energy into energy of resonance radiation. Thus, in the pioneer study,¹ a quasistationary plasma with an electron density $N_e \sim 10^{12} \text{ cm}^{-3}$ and an electron temperature

$T_e \sim 10^3 \text{ K}$ was formed upon irradiating Cs vapor at a pressure of 10^{-2} – 10^{-1} Torr with a cesium gas-discharge lamp. The radiation of the lamp corresponded to the spectral range $\lambda \geq 600 \text{ nm}$. The bulk of the energy of the radiation of the lamp was contained in the lines at $\lambda = 894.3$ and 852.1 nm , corresponding to the 6^2S – 6^2P resonance transitions. A detailed mass-spectrometric analysis showed¹ that the main type of ions in this plasma is the atomic ion Cs^+ . This indicates a complex character of the kinetics of ionization in the photoresonance cesium plasma; in particular, this implies that the process of associative ionization in the collision of two resonance-excited Cs atoms (6^2P) is not the fundamental ionization channel.¹ As is implied by the results of detailed experimental studies of recent years,^{3–5} the complex kinetics of ionization of atoms in the cesium photoresonance plasma includes processes of collision of two resonance-excited atoms,



processes of quenching of the excited Cs atoms (6^2P , 8^2P) by electron impact, processes of ionization of excited atoms in collisions with fast electrons formed as a result of quenching, processes of associative ionization, etc.

As the source of optical radiation for creating the photoresonance cesium plasma, not only cesium lamps, but also helium gas-discharge lamps have been successfully employed. This possibility arises from the coincidence of the wavelength of one of the effective transitions in the spectrum of He ($\lambda = 388.8 \text{ nm}$) with the wavelength of the 6^2S – 8^2P transition of the cesium atom. We note that this coincidence is the basis of one of the first schemes for excitation of a gas laser with optical pumping, which was proposed by F. A. Butaeva and V. A. Fabrikant¹⁶ and realized experimentally in Ref. 17. Using this scheme, a photoresonance cesium plasma was obtained with the parameters $N_{8^2\text{P}} \approx 10^7 \text{ cm}^{-3}$, $N_e \sim 10^8$ – 10^9 cm^{-3} , $T_e \sim 0.3 \text{ eV}$, $P_{\text{Cs}} \sim 10^{-3}$ – 10^{-2} Torr.¹⁸ In a plasma of this type, processes of stepwise excitation of highly excited levels from the 8^2P level by electron impact play an essential role. Figure 1 shows the dependences of the parameters of this plasma on the density of the Cs vapor with fixed intensity of resonance irradiation.

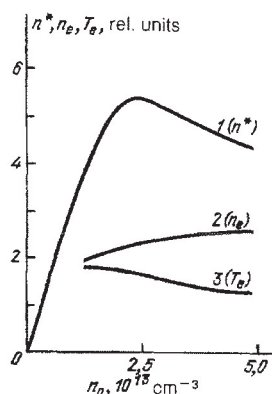


FIG. 1. Dependence of the parameters of a cesium plasma on the density of Cs vapor at fixed intensity of resonance irradiation.¹⁸ 1—density n^* of excited atoms ($\text{Cs}(8^2\text{P})$); 2—density n_e of electrons; 3—temperature T_e of electrons.

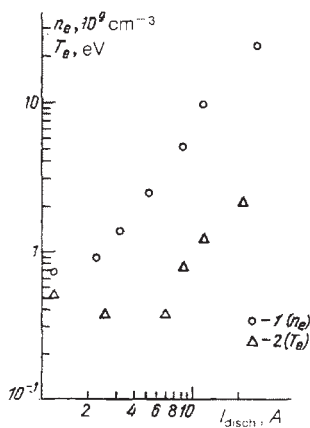
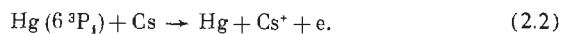


FIG. 2. Dependence of the concentration (1) and temperature (2) of the electrons of a photoresonance plasma in Hg vapor on the value of the discharge current in the optical-excitation source.²⁰

Mercury-vapor lamps are also an intense source of resonance radiation, and have been successfully used to create a photoresonance plasma in mercury vapor.^{19,20} Investigations in this direction were stimulated by practical problems of optical separation of mercury isotopes.²¹ Upon irradiating a gas-discharge mercury lamp with the resonance line corresponding to the transition $\text{Hg}(6^3P_1^0 \rightarrow 6^1S_0)$ ($\lambda = 253.7 \text{ nm}$), an increased concentration and a reduced temperature of the electrons was observed. This was associated with an increase in the efficiency of ionization under the action of the resonance radiation. The mercury lamp used as the source of resonance radiation had the form of a jacket arranged coaxially around the cylindrical cell being irradiated.²⁰ With a pressure of mercury vapor in the cell of $\sim 0.05 \text{ Torr}$, the concentration of Hg atoms in the $6^3P_1^0$ state reached 10^{11} cm^{-3} . The electrical characteristics of the photoplasma that was formed are shown in Fig. 2. Owing to the coaxial excitation geometry used in this experiment, a high degree of homogeneity of the photoresonance plasma was attained.

An interesting variety of photoresonance plasma was realized in Ref. 22, where a mixture of Hg and Cs vapors was irradiated with the resonance radiation of a mercury lamp ($\lambda = 253.7 \text{ nm}$). The ions were formed by the Penning reaction



According to the measurements performed using probe and

UHF diagnostics, at a concentration of $\text{Cs} \sim 3 \times 10^{15} \text{ cm}^{-3}$, $\text{Hg} \sim 3 \times 10^{13} \text{ cm}^{-3}$, and a pressure of buffer gas (Ar) $\sim 100 \text{ Torr}$, the photoresonance plasma was characterized by a density $N_e \sim 10^{12} \text{ cm}^{-3}$ and a temperature $T_e \approx 2000 \text{ K}$. The role of the buffer gas consists in reducing the effectiveness of the diffusion losses of charged particles, and hence, in maintaining the density of the electrons of the photoresonance plasma at a sufficiently high level. An analogous scheme for creating a photoresonance plasma was realized in Ref. 23, where a mixture of Cd and Cs vapors was irradiated with the resonance light of a cadmium lamp.

2.2. Photoresonance laser plasmas

The invention and wide spread of frequency-tunable narrow-band lasers based on dyes has stimulated to a considerable degree the study of the properties and possible applications of photoresonance plasmas. The set of studied objects has considerably expanded to encompass all the alkali metals, and also a number of metals of the second and third groups of the periodic table. The object of the studies was the mechanisms of ionization and recombination of particles of a plasma, the elucidation of the role of the buffer gas, the possibility of more complete extraction of ions in a photoresonance plasma and identifying them, etc.

Among the large number of experimental studies (see the review of the early studies⁹⁰) on the creation and study of photoresonance laser plasmas, primary attention is owed to a series of publications reporting the practically 100% ionization of metal vapors irradiated with the resonance radiation of a pulsed laser of relatively low power. Figure 3 shows a diagram of the first of these experiments, which was performed by Lucatorto and McIlrath.²⁴ The radiation of a dye laser pumped with a flash lamp was tuned to a line at $\lambda = 589.6 \text{ nm}$, which corresponds to the $3^2S_{1/2} - 3^2P_{1/2}$ transition of the Na atom, and was focused on a 10-cm column of Na vapor with addition of He to a total pressure about 1 Torr. The pulses of laser radiation of duration 500 ns had an energy of 300 mJ, which corresponds to a pulse power of 0.6 MW. The degree of ionization of the vapor was determined with a vacuum-ultraviolet spectrograph, which enabled measuring the absorption coefficient in the region $\lambda = 15-42 \text{ nm}$. Figure 4 shows typical densitograms of the spectrum obtained without (a) and with (b) laser irradiation. As is shown by comparison of the absorption coefficients in the region of $\lambda \approx 32.21 \text{ nm}$ corresponding to transitions of the Na^+ ion, the degree of ionization of Na during the laser pulse reaches 100%. The practically complete ionization of the Na vapor is also indicated by the sharp (by a factor of

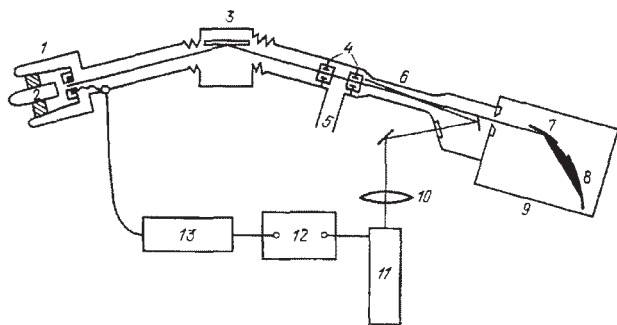


FIG. 3. Diagram of an experiment to produce and study a photoresonance sodium plasma with a high degree of ionization. 1—radiation source with a continuous spectrum; 2—anode; 3—toroidal mirror; 4—capillary rings; 5—vacuum pump; 6—furnace; 7—three-meter reflecting spectrograph; 8—diffraction grating; 9—photoplate; 10—cylindrical lens; 11—laser; 12—delay generator; 13—pulse shaper.

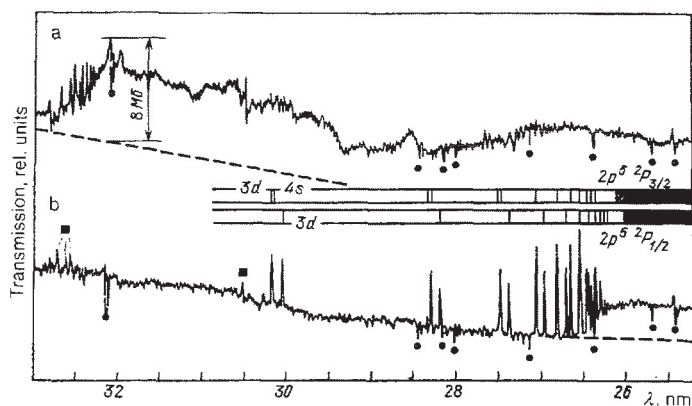
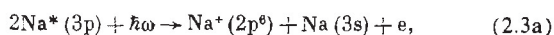
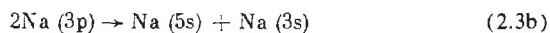


FIG. 4. Densitograms of the absorption spectrum of sodium.²⁴ a—Absorption of sodium vapor without irradiation; the dots indicate the emission lines of the vacuum arc, and the dotted line the absorption in He. b—Absorption of Na vapor irradiated with resonance laser radiation. The solid squares indicate the absorption lines of neutral Na.

10^6) decline in the absorption coefficient of the resonance laser radiation owing to the formation of the photoresonance plasma. Even the first rough estimates of the authors²⁴ indicated a complex, multistep mechanism of ionization of the vapor in the described experiments. Neither three-photon ionization nor radiation collision



nor multistep collisional excitation



with subsequent photoionization of the excited Na (5s) atoms possess values of the rate constants high enough to explain the observed 100% ionization of the atoms.

Analogous results were obtained in Ref. 25, where a cell filled with a mixture of Na vapor and Ar at a pressure of several Torr was irradiated with pulses of radiation of a dye laser based on rhodamine 6G pumped with a nitrogen laser. The radiation pulses of 100 kW power had a duration of 10 ns and a line width ~ 0.1 nm. The ionization of the gas was measured by the magnitude of the photocurrent, for which a typical dependence on the Na vapor density is shown in Fig. 5. Figure 6 shows the dependence of the electron temperature on the time elapsed since the end of the laser pulse, as obtained by the Langmuir double-probe method. The results of the probe measurements of the electron density performed at a point separated by 2 mm from the focus of the laser beam are shown in Table I.

The effect described above of intense ionization of va-

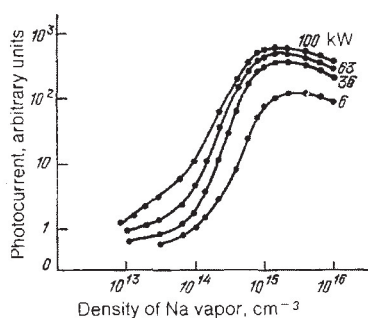


FIG. 5. Dependences of the photocurrent on the density of Na vapor obtained at different levels of laser power.²⁵

pors under the action of resonance laser radiation has been observed in subsequent experiments with vapors of Li,²⁶ Cs,²⁷ Ca,²⁸ Sr,²⁹ Ba,²⁸⁻³⁴ Na,³⁵ and Mg.³⁶ The properties of the PRP formed thereby have been studied in greatest detail in Ref. 36, where Mg vapor was irradiated with radiation corresponding to the resonance transition $3^1S_0 \rightarrow 3^1P_1$ ($\lambda = 285.2$ nm) of the singlet system of levels. A pulsed liquid dye laser with frequency doubling pumped with the second harmonic of a neodymium laser with a pulse repetition frequency of 3 Hz was used as the radiation source. The pulses of ultraviolet radiation had a line width ~ 0.1 cm⁻¹, and duration ~ 10 ns at a power ~ 1 kW. Another liquid laser ($\lambda = 280.3$ nm) tuned to the transition $3^2P_{1/2} - 3^2S_{1/2}$ of the Mg⁺ ion was used to measure the concentration of Mg⁺ ions. In addition, the experiment measured the luminescence of the Mg vapor and the time-dependence of the photocurrent. The pulse of the probe radiation had a delay with respect to the pump pulse variable in the range up to 100 μ s. Figure 7 shows a diagram of the experiment.³⁶

The experimental chamber, which was made of stainless steel and fitted with quartz windows and internal plane electrodes to measure the photocurrent, was filled with an inert gas at a pressure ~ 1 Torr. The pressure of metal vapor (Mg) was varied in the range 0.1–1.0 Torr. Upon tuning the pump radiation to the frequency of the resonance transition

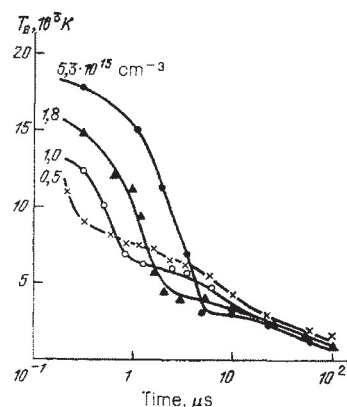


FIG. 6. Dependences of the electron temperature on the time elapsed after cessation of the laser radiation pulse.²⁵ The curves are marked with the different values of the concentration of Na vapor.

TABLE I. Values of the electron density N_e in a photoresonance plasma measured at different values of the density of Na vapor.²⁵

| | | | | |
|---------------------------------|---------------------|---------------------|---------------------|---------------------|
| $N_{\text{Na}}, \text{cm}^{-3}$ | $5,9 \cdot 10^{14}$ | $1,0 \cdot 10^{15}$ | $1,8 \cdot 10^{15}$ | $5,3 \cdot 10^{15}$ |
| N_e, cm^{-3} | $6,6 \cdot 10^{12}$ | $9,5 \cdot 10^{12}$ | $1,0 \cdot 10^{13}$ | $7,0 \cdot 10^{12}$ |

of Mg, an emission from the Mg vapor arose in the region of the laser-beam focus at frequencies corresponding to transitions $n^1D_2-3^1P_1$ ($n = 4-10$) of the singlet system and n^3S-3^3P ($n = 4, 5$) of the triplet system of Mg levels. Here the absence was noted of radiation at the strong line $5^1S_0-3^1P_1$ ($\lambda = 571.1 \text{ nm}$) and several other strong lines. As was shown by measurements of the density of Mg ions performed with probe radiation, the maximum concentration of ions ($\sim 2 \times 10^{14} \text{ cm}^{-3}$) was observed about 30 ns after the end of the pulse of pump radiation, while the total time of existence of the PRP amounted to $\sim 10 \mu\text{s}$. The maximum degree of ionization of the plasma reached 5%. The absence of saturation in the dependence of the ion density on the intensity of pump radiation allows one to expect an increase in the PRP density upon using more intense resonance pump radiation.

Another detailed study worthy of attention on the character of formation and physical properties of a PRP with a rather high degree of ionization was performed by the authors of Ref. 35, where a dye laser (rhodamine C) was used as the source of resonance radiation. It was pumped with the radiation of the second harmonic of a solid-state pulsed laser based on yttrium aluminum garnet of type LTIP4-5 with a pulse-repetition frequency of 12.5 Hz. To narrow and tune smoothly the emission line of the dye laser, a diffraction grating (1200 lines/mm) was used and was set up in a glancing-incidence system. The width of the emission line of this laser amounted to $\sim 1 \text{ nm}$, and the emission power was $\approx 40 \text{ kW}$ at a pulse duration of $\sim 10^{-8} \text{ s}$. The laser was tuned either to the resonance transition of Na ($\lambda = 589.0 \text{ nm}$) or to the wavelength 578.7 nm corresponding to two-photon absorption to the excited state of Na ($4d^2D_{5/2}$).

The Na vapor diluted with inert gases filled the discharge tube, which was made of Pyrex and had niobium tubular electrodes. The pressure of the vapor in the tube was maintained by using a heating element. Under the conditions

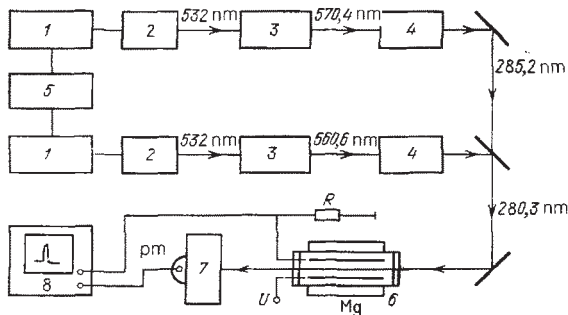


FIG. 7. Diagram of an experimental arrangement to form a quasiresonance laser plasma in Mg vapor.³⁶ 1—neodymium garnet laser; 2, 4—frequency doublers based on KDP; 3—dye laser; 5—delay circuit; 6—cell with Mg vapor; 7—monochromator with photomultiplier (PM); 8—oscillograph.

of the experiment one pulse of laser radiation contained about 5×10^{14} photons. About the same number of Na atoms was contained in the irradiated volume. Here conditions were selected such that, on the one hand, practically complete absorption of the laser radiation was attained, and on the other hand, the intensity of absorption varied weakly along the laser beam. This was made possible by detuning the frequency of the laser beam from the center of the absorption line by four widths of the Doppler absorption contour (equal to 0.0024 nm). Whereas at the center of the absorption line the optical density of the medium amounted to $\sim 10^6$, at the detuned frequency it was close to unity.

The formation of a PRP was measured from the change in electrical conductivity of the irradiated volume. To do this, a voltage was applied to the electrodes of the discharge tube smaller than the excitation voltage of the discharge, and the current was measured that arose in the electrical circuit under the action of the laser illumination. Figure 8 shows an oscillogram of this current obtained at a voltage on the electrodes of 100 V and a vapor pressure of Na of 3×10^{-3} Torr. The pressure of the buffer gas amounted to 1 Torr. As the pressure of Na vapor was increased from 3×10^{-4} Torr to 0.2 Torr, the magnitude of the signal and its duration increased by more than an order of magnitude. Upon detuning from the resonance at $\lambda = 589 \text{ nm}$, no plasma formation was observed.

Plasma formation was also observed in two-photon laser excitation of the level $4p^2D_{5/2}$. The oscillograms of the current obtained here at a pressure of Na vapor $\sim 5 \times 10^{-3}$ Torr are shown in Fig. 9. The rapidly growing advance front of the current pulse was associated³⁵ with the phenomenon of three-photon ionization of atoms via a two-photon resonance, and the subsequent, smoother increase in electrical conductivity—with a supplementary mechanism of formation of free electrons (heating of electrons by superelastic processes and subsequent ionization of atoms by electron impact).

As an analysis of the experiments to create and study a laser PRP shows, a plasma of rather high density is formed using very-low-power laser radiation. This arises from the high absorption power of gases for resonance radiation, and also the high efficiency of conversion of the energy of resonance-excited atoms into ionization energy.

2.3. Quasiresonance plasmas

As has been established in a number of experiments of recent years,^{13,29,37} to form a photoresonance plasma one need not use radiation whose frequency corresponds to a resonance transition between the ground and excited states of the atom. Efficient ionization of the atoms of a metal vapor has also been observed using radiation corresponding to a transition between two excited states of the atom. Here the intensity of the laser radiation was not so great that one

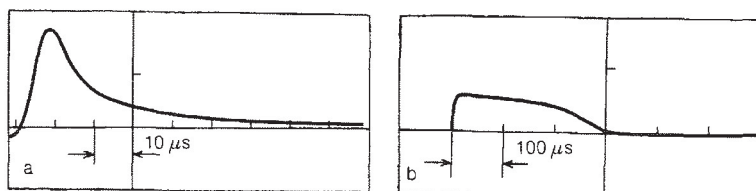


FIG. 8. Oscilloscope of the photocurrent that arises upon irradiating a discharge tube containing a mixture of Na + Ne with a pulse of laser radiation ($\lambda = 589 \text{ nm}$),³⁵ in the presence of a discharge (a), and at a voltage below that for ignition of the discharge (b).

could ascribe such an unexpected result to effects of multiphoton ionization of atoms, including the nonresonance excitation of a real level.³⁸

A plasma of the type being studied has been called a "quasiresonance laser plasma." As has been established by detailed experimental studies, to form a quasiresonance plasma one can use radiation at one of many frequencies corresponding to transitions between excited states of the atom. Thus, a quasiresonance cesium plasma was efficiently formed upon irradiating Cs vapor with laser radiation having $\lambda = 583.9, 601.0, 603.5,$ and 621.3 nm , corresponding to the transitions $^2S_{1/2}10s \rightarrow ^2P_{1/2}^0 6p$, $^2D_{3/2} 8d \rightarrow ^2P_{1/2}^0 6p$, $^2S_{1/2}10s \rightarrow ^2O_{3/2}^0 6p$, and $^2D_{3/2}8d \rightarrow ^2P_{3/2}^0 6p$, as well as when using radiation at several other transitions of the atom.¹³ Here the formation of the quasiresonance plasma has a threshold character—this phenomenon is observed only upon exceeding certain values of the pressure of the vapor and intensity of the laser radiation.

Another interesting feature of a quasiresonance laser plasma involves the relatively low level of intensity of radiation used to maintain it. Thus, in the series of studies cited above,¹³ continuous irradiation of cesium vapor of density $\sim 3 \times 10^{17} \text{ cm}^{-3}$ with quasiresonance radiation of power up to $\sim 100 \text{ mW}$ yielded a plasma with a degree of ionization of 10^{-3} . A diagram of the experiment is shown in Fig. 10. As is shown by analyzing photographs of the plasma column formed upon focusing the beam of a continuous laser of 10 mW power, the extent of the column amounts to about 4 mm and the diameter to less than 1 mm . Even weaker radiation was used in Ref. 37 to maintain a plasma in Na vapor. This radiation having a power of $\sim 2 \text{ mW}$ was tuned in resonance with the 3p-4d transitions ($\lambda = 568.8$ or 568.2 nm) of the Na atom. The pressure of the Na vapor amounted to $\sim 10 \text{ Torr}$. Detailed spectral studies of the plasma that was formed led the authors to conclude that the decisive role in forming the plasma was played by the process of associative ionization involving a (4d) Na atom.

The mechanism of ionization of a gas under the action of quasiresonance radiation¹³ includes the process of photodissociation of dimers of a metallic vapor, which are always present in the system:

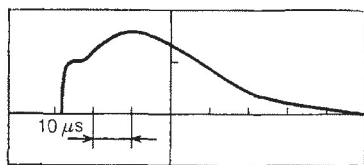
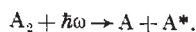


FIG. 9. Oscilloscope of the photocurrent observed in two-photon laser excitation of Na vapor ($\lambda = 578.9 \text{ nm}$).³⁵

One of the atoms formed as a result of photodissociation of the dimer exists in the excited state (in the case of Cs this state is $6p^2P_{1/2,3/2}$), and is already capable of resonance absorption of laser radiation. This leads to formation of highly excited atoms, whose ionization results from subsequent collisional processes.

2.4. Beam and jet photoresonance plasmas

The most productive way to study the primary starting mechanisms responsible for the formation of a PRP involves using atomic beams. In this case one can reduce to a minimum the role of secondary collisional processes and isolate in pure form the process that occurs with participation of optically excited atoms and leads to their ionization. A characteristic example of such an experiment is Ref. 39, where an effusion beam of Na atoms was irradiated with a dye laser tuned to a resonance transition while pumped with an argon ion laser. The density of atoms in the irradiated zone amounted to 10^9 cm^{-3} , the intensity of the laser radiation was 0.5 W/cm^2 , and the line width was 20 MHz . The positive ions were extracted from the interaction region with a pair of electrodes to which a potential was applied, and which created an electrical field in the cell. Then the ions entered the input of a quadrupole mass spectrometer. This made it possible to establish that only molecular Na_2^+ ions are formed under the conditions of the experiment. As was shown by comparing the results of the mass-spectrometric measurements with those of relative measurements of the concentration of resonance-excited atoms based on the fluorescence of the beam, a proportional relation is observed between the yield of Na_2^+ ions and the square of the density of excited Na atoms. This enabled concluding that the decisive role is played by the process of associative ionization



and establishing the value of the rate constant of this process ($\sim 1.5 \times 10^{-13} \text{ cm}^3/\text{s}$) and its cross section ($\sim 0.5 \times 10^{-17} \text{ cm}^2$).¹¹

A higher intensity of ionization using resonance radiation was obtained in a jet experiment,⁴⁰ in which a beam of monoenergetic Cs^+ ions was formed in this way. A glass

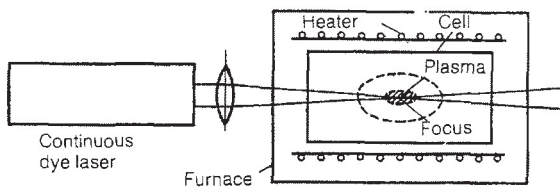


FIG. 10. Diagram of an experiment to form a quasiresonance laser plasma using a continuous-wave dye laser.¹³

chamber maintained at a constant temperature in the range 400–500 K (pressure of Cs vapor $\sim 2 \times 10^{-3}$ –0.2 Torr) and equipped with a nozzle 0.12 mm in diameter was used as the source of the cesium vapor. Thus a jet of vapor was formed that was concentrated in a solid angle $\theta = 2.7 \times 10^{-2}$ steradian and characterized by an intensity of 8.6×10^{11} atoms/s and a mean energy of the atoms of ~ 0.06 eV. The energy spread of the atoms in the jet was of the same order of magnitude. This corresponds to a density of Cs atoms near the critical cross section of the nozzle of $\sim 10^{12}$ cm $^{-3}$. The ionization of the Cs atoms was carried out in two stages. In the first stage the resonance radiation of a semiconductor injection CaAlAs laser was used ($\lambda = 852.1$ nm), which converted the Cs atoms to the $6^2P_{3/2}$ state. In the second stage the radiation of an argon ion laser was used ($\lambda = 488.0, 496.5,$ and 501.7 nm), which enabled the photoionization of the resonance-excited atoms. Figure 11 shows the dependence of the photocurrent on the extracting potential. According to the estimates the flux of ions in the jet reached values of 10^8 s $^{-1}$. A substantial increase in this parameter was obtained in a subsequent study by this same author,⁴⁰ where values were reached of $\sim 10^{12}$ s $^{-1}$ with an energy spread of the ions at the level of 0.15 eV.

Two-stage and multistage photoionization of atoms has been used successfully to obtain beams of the following ions: Ca $^+$,⁴¹ In $^+$ (under the action of dye-laser radiation),⁴² Al $^+$ (using the radiation of an excimer XeCl laser),⁴³ etc.^{13,15} The ion beams thus formed were characterized by being highly monoenergetic and by a degree of purity unattainable when using other methods of forming an ion beam. Here, as in the studies cited above, the obtainable ion fluxes were relatively small, so that problems of extracting the positive ions from the photoresonance plasma did not arise. Further increase in the efficiency of ionization of atoms in atomic beams and jets can lead to the appearance of the effects of Debye screening, which hinders the penetration of the electric field into the photoresonance plasma and restricts the magnitude of the limiting ion current extractable from the plasma. The stated limitations have been analyzed in detail in Ref. 44.

3. ELEMENTARY PROCESSES IN A PHOTORESONANCE PLASMA

3.1. Photoprocesses

A photoresonance plasma is created and controlled by a group of elementary processes, which we shall proceed to discuss.

The first of them is the absorption of the resonance radiation, which leads to creating a high concentration of excited atoms. Collision of the excited atoms with one another yields highly excited atoms, and also ions and electrons. Subse-

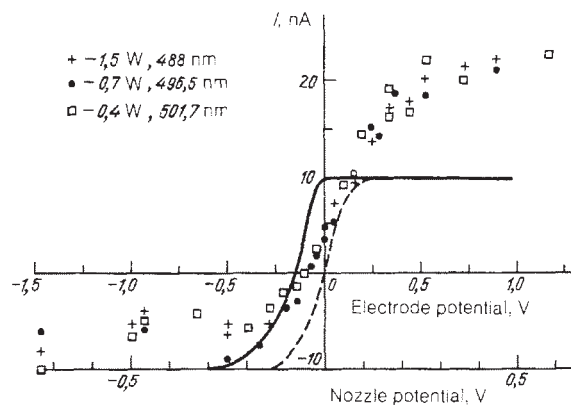


FIG. 11. Dependences of the photocurrent of Cs $^-$ ions on the extracting potential obtained using a continuous-wave laser of varying power and wavelength.⁴⁴

quent collisions of the electrons that are formed with excited and unexcited atoms establishes an equilibrium over the excited states of the atoms, and also an equilibrium between the excited states of the atoms and the states of the continuous spectrum. The energy losses of the photoresonance plasma involve its emission in the resonance lines. We shall proceed to examine all these elementary processes.

The features of the photoprocesses in a photoresonance plasma consist in the fact that the mean free path of the resonance photons is relatively small, so that reradiation processes play a great role.⁴⁵ At not very high densities of atoms the broadening of the resonance line is governed by collisions of atoms in the excited state with atoms in the ground state. The broadening arises from the dipole-dipole interaction, with a substantial contribution to the cross section of this process coming from excitation transfer. Table II gives the parameters of the broadening of the spectral line for the S–P transition as calculated in Refs. 46–48. The width of the line is given in units of $\pi N g^2 / \hbar$, where N is the density of atoms in the ground state, and the quantity g^2 is given by the relationship

$$g^2 = \frac{1}{2j+1} \sum_{m, m_0} | \langle j_0 m_0 | \mathbf{D} | j m \rangle |^2. \quad (3.1)$$

Here j_0 and m_0 are the angular momentum and its projection on a chosen direction for the ground state of the atom, and j and m are the same parameters for the excited state of the atom. \mathbf{D} is the operator for the dipole moment of the atom.

Table III gives the values of the parameter g^2 for a number of atoms and indicates the resonance-excited state for which the cited value corresponds to a transition from the ground state.⁴⁹ This table also gives the wavelengths of the transitions and the lifetimes of the studied excited states.⁵⁰

TABLE II. Width of resonance line (in units of $\pi N g^2 / \hbar$).

| | | | | | |
|------------------------|--------|-------------------|------------|--------|--------|
| Ground state | $1S_0$ | $2S_{1/2}$ | $2S_{1/2}$ | $3S_1$ | $3S_1$ |
| Excited state | $1P_1$ | $2P_{1/2}$ | $2P_{3/2}$ | $3P_1$ | $3P_2$ |
| Width of spectral line | 2.41 | 1.2 ¹⁾ | 1.86 | 1.4 | 1.8 |

TABLE III. Parameters of transitions to resonance-excited states.

| Excited state of atom | H (2 2P) | He (2 1P) | Li (2 2P) | Na (3 2P _{1/2}) | Na (3 2P _{3/2}) | Mg (3 1P ₁) | K (4 2P _{1/2}) | K (4 2P _{3/2}) | Ca (4 1P ₁) |
|--------------------------------|-------------------------|---------------------------|---------------------------|---------------------------|---------------------------|---------------------------|---------------------------|--------------------------|-------------------------|
| Wavelength λ , nm | 121,57 | 58,43 | 670,8 | 589,6 | 589,0 | 285,2 | 769,9 | 766,5 | 422,7 |
| Lifetime τ , ns | 1,60 | 0,555 | 27,3 | 16,4 | 16,3 | 2,1 | 27 | 27 | 4,6 |
| g^2 , a. u. | 0,555 | 0,177 | 3,65 | 6,28 | 6,28 | 3,76 | 8,80 | 8,63 | 6,94 |
| k_0 , 10^5 cm^{-1} | 13 | 18 | 3,6 | 1,2 | 1,5 | 5,3 | 0,86 | 1,1 | 2,9 |
| Excited state of atom | Zn (4 1P ₁) | Rb (5 2P _{1/2}) | Rb (5 2P _{3/2}) | Sr (5 1P ₁) | Cd (5 1P ₁) | Cs (6 2P _{1/2}) | Cs (6 2P _{3/2}) | Ba (6 1P ₁) | Hg (6 1P ₁) |
| Wavelength λ , nm | 213,9 | 794,8 | 780,0 | 460,7 | 228,8 | 894,4 | 852,1 | 553,6 | 185,0 |
| Lifetime τ , ns | 1,4 | 28,5 | 26,5 | 6,2 | 1,7 | 31 | 31 | 8,5 | 1,3 |
| g^2 , a. u. | 2,82 | 9,48 | 9,32 | 7,79 | 3,01 | 11,6 | 11,6 | 8,5 | 2,44 |
| k_0 , 10^5 cm^{-1} | 6,0 | 0,81 | 1,1 | 2,3 | 5,3 | 0,77 | 0,90 | 2,2 | 5,6 |

The presented parameters allow one to determine the cross sections for the absorption and emission of a photon, and also the absorption coefficient. The absorption cross section at a frequency ω close to resonance is^{51,52}

$$\sigma_\omega = \frac{\lambda^2}{4\tau} a_\omega \frac{g_b}{g_0}$$

Here λ is the wavelength of the radiation, τ^{-1} is the probability of spontaneous emission for the given transition, a_ω is the shape of the absorption line, and g_0 and g_b are the statistical weights of the levels taking part in the transition.

Whenever the broadening of the line of the transition arises from collisions with individual atoms, the shape of the absorption line is

$$a_\omega = \frac{\Delta\omega}{2\pi} \left[(\omega - \omega_0)^2 + \left(\frac{\Delta\omega}{2} \right)^2 \right]^{-1} \quad (3.2)$$

Here ω_0 is the frequency corresponding to the center of the line and $\Delta\omega$ is the width of the line. For a photoresonance plasma with real parameters, the transport of radiation is governed precisely by this mechanism. Here the line width itself can be determined by a Doppler broadening mechanism. For example, in the case of sodium vapor at a vapor temperature of 1000 K, the widths of the lines arising from impact and Doppler broadening mechanisms are comparable for a transition to the resonance $3^2P_{1/2}$ state at a density of atoms in the vapor of $7 \times 10^{16} \text{ cm}^{-3}$, and for the transition to the state $3^2P_{3/2}$ at a density of atoms of $5 \times 10^{16} \text{ cm}^{-3}$. However, since in photoprocesses in an optically dense vapor the essential contribution comes from the tails of the lines, Doppler broadening is not significant, even for lower densities of atoms.

Upon taking account of Eqs. (3.1) and (3.2) and the data of Table II, we can represent the expression for the absorption coefficient at the center of the line in the form

$$k_0 = N\sigma(\omega = \omega_0) = \frac{\lambda^2}{4\pi^2\tau g^2 b} \frac{g_b}{g_0} (1 - e^{-h\omega/T}) \quad (3.3)$$

Here the values of the coefficient b are given in Table II, and T is the temperature corresponding to the occupancy of the excited states. Since the concentration of excited atoms in the photoresonance plasma is higher than in the gas-discharge plasma, the factor that includes the temperature of

the excited atoms is more substantial for the photoresonance plasma. Table III gives the values of the absorption coefficient at the center of the line for a set of transitions in the limit where $h\omega \gg T$, at which the expression in parentheses in Eq. (3.3) equals unity. We note that the impact theory of broadening for which these data are given is valid when the following criterion holds^{51,52}:

$$\frac{\bar{v}}{\sigma_{\text{tot}}^{1/2}} \gg \Delta\omega \gg \frac{1}{\tau} \quad (3.4)$$

Here $\Delta\omega$ is the frequency shift with respect to the center of the line, τ is the radiative lifetime of the excited state, \bar{v} is the thermal velocity of motion of the atoms, and σ_{tot} is the total scattering cross section for collision of atoms in the ground and excited states.²⁾ The right-hand inequality indicates that the impact width considerably exceeds the natural width of the line arising from the finite lifetime. When it is violated the absorption coefficient for a photon at the center of the line depends on the density of the gas, and at low gas density is proportional to it. We note that we have $\Delta\omega = 1/\tau$ for Na ($3^2P_{1/2}$) at a density of sodium atoms of $4 \times 10^{14} \text{ cm}^{-3}$.

When the left-hand inequality of (3.4) is violated, we should use the quasistatic theory instead of the impact theory of broadening. However, this has no significance in principle, since the dependence of the shape of the emission line a_ω in the tail of the line on the density of atoms and frequency of the photons is the same in both cases.

The obtained results can be used to determine the power lost by the photoresonance plasma in emission. The probability for a resonance photon to travel a distance d without being absorbed is proportional to $(k_0 d)^{-1}$, where k_0 is the absorption coefficient at the center of the line. Hence we obtain an expression for the flux of photons emitted by the photoresonance plasma⁵³:

$$j = a \frac{N_b d^{1/2}}{\tau k_0^{1/2}} \quad (3.5)$$

Here a is a numerical coefficient, N_b is the density of excited atoms, and d is the distance between the boundaries of the plasma in a plane geometry or the diameter of the cylinder restricting its volume. In the case in which the plasma lies between infinite parallel planes, we have $a = 0.376$. If it oc-

copies the volume of an infinite cylinder, we have $a = 0.274$, while if it lies inside a sphere we have $a = 0.226$.⁵³

3.2. Collision of electrons with excited atoms

Processes of collision of electrons with atoms play an important role in a photoresonance plasma. The temperature and density of the electrons are established by collisions of the electrons with atoms in the ground and resonance-excited states, and also by the subsequent processes of excitation and ionization of the resonance-excited atoms. Let us examine these processes.

First let us study the quenching of the excited state by electron impact. The essential point is that the rate constant of this process does not depend on the energy of the electron, since the energy ε of the electron is much smaller than the excitation energy $\Delta\varepsilon$.⁵⁴ Actually this rule is valid also when $\varepsilon \sim \Delta\varepsilon$. Let us employ a simple representation⁵⁵ for the rate constant for excitation of the resonance state of the atom by electron impact, which requires that the excitation cross section should correspond to the Born approximation at large energies, and to the set of experimental data in the threshold energy region. Then we can represent the rate constant for quenching of the resonance-excited state in the form^{55,56}

$$k_{\text{quench}} = \frac{k_0}{\tau \Delta\varepsilon^{7/2}}, \quad T_e \ll \Delta\varepsilon. \quad (3.6)$$

Here τ is the radiative lifetime of the excited state, and k_0 is a universal constant. Table IV gives the values of the rate constants for quenching of the atoms of the alkali metals by electron impact as measured and calculated⁵⁷⁻⁵⁹ in the temperature range up to 1 eV. These data are averaged over the values pertaining to different temperatures and different measurements and calculations. If τ in Eq. (3.6) is measured in 10^{-8} s, and $\Delta\varepsilon$ in eV, the value thus obtained of the parameter k_0 in Eq. (3.6) amounts to $(4.6 \pm 0.7) \times 10^{-6}$ cm³/s. The rate constant for excitation by electron impact can be derived from the rate constant for quenching on the basis of the principle of detailed balancing.

One can make a sufficiently reliable determination of the rates of ionization and recombination in a photoresonance plasma under certain conditions that are imposed on the parameters of the plasma. On the one hand, the density of electrons in the plasma must be high enough that the ionization is stepwise in character, and on the other hand, the temperature of the electrons must be relatively low, so that many excited states of the atom participate in the processes of ionization and recombination. Under these conditions the theory of a nonequilibrium plasma^{45,60,61} holds true, according to which

$$\frac{\alpha}{N_e} = \frac{\mathcal{K}_0}{T_e^{3/2}}, \quad K_{\text{step}} = \frac{g_e g_i}{g_a} \frac{\alpha}{T_e^3} e^{-J/T_e}. \quad (3.7)$$

Here g_e , g_i , and g_a are respectively the statistical weights of an electron, an ion, and an atom, J is the ionization potential of the atom, $\mathcal{K}_0 = (1.0 \pm 0.3) \times 10^{-26}$ cm⁶eV^{9/2}/s, and $\alpha = (3.1 \pm 0.9) \times 10^{-5}$ cm³eV³/s. The stated limits of error allow for the degree of agreement of the results of calculations of the recombination coefficients performed for different models. We note that K_{step} can pertain also to the stepwise ionization of an excited atom. We shall use the presented information later on in analyzing the kinetics of a photoresonance plasma.

TABLE IV.

| Atom | $k_{\text{quench}}, 10^{-7}$ cm ³ /s | $k_0, 10^{-14}$ cm ³ eV ^{7/2} |
|-----------------------|---|---|
| K (4 ² P) | 3,2±0,4 | 4,6±0,6 |
| Rb (5 ² P) | 3,4±0,5 | 4,7±0,7 |
| Cs (6 ² P) | 4,1±0,7 | 4,5±0,8 |

3.3. Ionization with participation of excited atoms

A photoresonance plasma maintained with the aid of resonance radiation is not in equilibrium. The density of excited atoms in it exceeds its equilibrium value corresponding to the given value of the electron temperature. In such a situation an important role in forming the plasma is played by processes that involve excited atoms. One of these processes, which was discussed in detail above, is the quenching of excited atoms by electron impact, which pumps the energy of the resonance radiation over into the energy of free electrons. The electrons heated in this way can then collide with excited or unexcited atoms to excite or ionize them. Another type of processes that play a substantial role in the reprocessing of the energy of resonance radiation into ionization energy is collisional ionization with participation of excited atoms:



The first of the two processes written here is called the Penning process, and the second, associative ionization. The results of detailed experimental studies of these processes have been presented in many publications (see, e.g., Refs. 3, 54, 56, 62, 63).

The occurrence of process (3.8b) requires less internal energy of the atoms than for occurrence of process (3.8a). Therefore the process of associative ionization is manifested over a broader region of conditions of the photoresonance plasma than the Penning process. To estimate the possibility and efficiency of occurrence of the process of associative ionization, one can establish the sign and magnitude of the energy defect of this process, defined as the difference of internal energies of the initial and final states of the system:

$$\delta\varepsilon = J(A) - D(A_2^+) - 2\Delta\varepsilon.$$

Here $J(A)$ is the ionization potential of the atom, $D(A_2^+)$ is the binding energy of the molecular ion, and $\Delta\varepsilon$ is the resonance excitation energy of the atom. In the case of atoms of the inert gases the quantity $\delta\varepsilon$ has a large negative value. Hence the ionization cross section proves to be of the order of magnitude of the capture cross section in the collision of two excited atoms.⁶²

From the standpoint of creating a photoresonance plasma, we are more interested in the vapors of the alkali metals. Table V presents the values of $\delta\varepsilon$ calculated for atoms of this type.

As we see, for all atoms except Na, the excitation energy of two atoms is insufficient for ionization. However, even in the case of Na, the process requires overcoming a potential barrier (Fig. 12⁶⁴) of height $\Delta U = 0.11 \pm 0.02$ eV.⁶⁴ This explains the sharp temperature dependence of the rate con-

TABLE V. Values of the quantity $\delta\epsilon = J(A) - D(A_2^+) - 2\Delta\epsilon$ for alkali-metal atoms.

| Excited atom | Li (2 2P) | Na (3 2P) | K (4 2P _{1/2}) | Rb (5 2P _{1/2}) | Cs (6 2P _{1/2}) |
|-----------------------|-----------|-----------|--------------------------|---------------------------|---------------------------|
| $\delta\epsilon$, eV | 0,39 | -0,002 | 0,32 | 0,36 | 0,48 |

stant of the process $2Na(3p) \rightarrow Na_2^+ + e$, and also the high sensitivity of this parameter to the form of the velocity distribution function,⁶⁵ which is manifested in a scatter of the results of different experiments over a range of two orders of magnitude.^{38,66,67}

What we have said implies that ionization in the photoresonance plasma of an alkali metal requires the presence of excited atoms (A^{**}) having an excitation energy appreciably exceeding the energy of the resonance transition. These atoms can be formed in pair collisions of resonance-excited atoms:



The rate constant of process (3.9) for characteristic energies of the atoms in the photoresonance plasma agrees in order of magnitude with the rate constant for capture in collision of excited atoms. That is, it proves to be of the order of 10^{-10} – 10^{-9} cm³/s.

Subsequent collisions of the highly excited atoms A^{**} with resonance-excited atoms A^* leads to ionization by the mechanism (3.8a) or (3.8b). Here the magnitude of the rate constant of Penning ionization in (3.a) with participation of excited (A^*) and highly excited (A^{**}) atoms is given by the relationship⁵⁴

$$k_{ion} = b \frac{J^*}{\Delta\epsilon^2} f^{2/5}. \quad (3.10)$$

This is valid if the process occurs with long free paths of the atoms, for which elastic scattering is inessential.³¹ Here the parameter b is 1.6×10^{-6} cm³eV/s, J^* is the ionization potential of the highly excited atom A^{**} , $\Delta\epsilon$ is the energy of resonance excitation of the atom A^* , and f is the oscillator strength of the resonance transition. As we see, the quantity k_{ion} is $\sim 10^{-7}$ – 10^{-6} cm³/s, which considerably exceeds the rate constant of the process (3.9). Therefore the stepwise excitation in the collision of two excited atoms usually leads to rapid, practically instantaneous ionization of the highly excited atom A^{**} .

As we noted above, the associative ionization of (3.8b) practically does not occur in the collision of resonance-excited atoms of the alkali metals, which involves an energy deficit. The cross section for associative ionization increases with increasing excitation energy of the atom. In the case of highly excited atoms with a binding energy of the electron

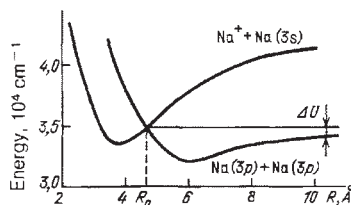


FIG. 12. Potential curves of the states of Na_2 that participate in the process of associative ionization.⁶⁴

smaller than, or of the order of, the dissociation energy of the molecular ion $D(A_2^+)$, associative ionization can occur in the collision of a highly excited atom with an unexcited atom:



The stated process occurs efficiently upon approach of the nuclei to a distance much smaller than the dimension of the highly excited atom, but much greater than that of the unexcited atom.

At the instant of transition the valence electron lies far from the close-lying atom and ion. Hence the characteristics of the process substantially depend on the binding energy of the weakly bound electron and are weakly sensitive to the type of the atom A . A theoretical model of the process of associative ionization of (3.11) based on these features has been developed.^{68,69} According to the theory, associative ionization arises from photodetachment of the weakly bound valence electron, which results from the transition of the molecular ion from a repulsive, odd term to an attractive, even term. Figure 13 compares the dependences of the rate constant of the process (3.11) for Na on the effective value of the principal quantum number n^* calculated on the basis of this theory with the results of measurement.⁷⁰ Analogous dependences have been obtained experimentally also in Refs. 71, 72 (Rb), Refs. 73–75 (Na), Ref. 76 (Ba), Ref. 77 (Li), and Ref. 78 (Cs). These dependences are characterized by the existence of a maximum in the region $n^* \approx 10$, where the rate constant of associative ionization acquires values $\sim 10^{-9}$ – 10^{-8} cm³/s, and by a decline by the law $k \sim (n^*)^{-3}$ in the region $n^* > 15$. Here, since the radiative lifetime of a highly excited atom is characterized by the relationship $\tau \sim n^{*3}$, the ratio of the number of atoms undergoing associative ionization to the number of atoms (in a given highly excited state) that decay by spontaneous emission is proportional to the product $k\tau$ and proves to be independent

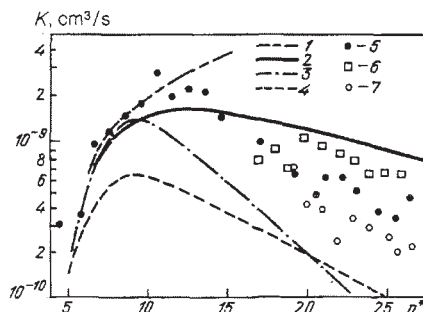


FIG. 13. Dependences of the rate constant of associative ionization $Na(n^*, l) + Na(3s) \rightarrow Na_2^+ + e$ on the effective value of the principal quantum number n^* , as calculated from the model⁶⁸ and as measured.⁷⁰ Theory: 1—overall constant; 2— $l=1$; 3— $l \geq 2$; 4— $l=0$. Experiment: 5— $l=1$; 6— $l=0$; 7— $l \geq 2$.

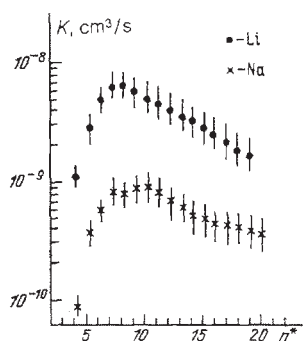


FIG. 14. Rate constant of associative ionization of atoms of Li⁷⁷ ($T = 100$ K) and Na⁷⁵ ($T = 1000$ K) as a function of the effective value of the principal quantum number n^* .

of the magnitude of n^* . The stated ratio increases with increasing pressure of the vapor. At high enough pressures (usually this corresponds to a vapor density $N \geq 10^{14}$ cm⁻³), spontaneous emission becomes inessential, so that all atoms excited to a state having the given value of the effective principal quantum number $n^* > 15$ undergo associative ionization.⁷⁴

The maximum value of the rate constant of associative ionization observed in experiments reaches values $\sim 10^{-8}$ cm³/s in the case of Li.⁷⁷ The results of this experiment are compared in Fig. 14 with the results obtained by the same authors for Na.⁷⁵

Another effective mechanism of collisional ionization of excited atoms is realized in the case of collision of a highly excited atom with an electronegative atom or molecule. Here ionization can occur with formation of positive and negative ions. In the case of the alkali metals, whose atoms possess an electron affinity, the stated mechanism can be realized in a one-component gas⁷⁹⁻⁸¹:



The results of measurements of the rate constant of the process (3.12) for different states of the Rb atom are given in Table VI.⁸⁰

A somewhat higher value of the cross section than in the cited case of Rb is given in Ref. 81, where the process (3.12) was studied when occurring with participation of a highly excited Na atom ($n = 7$). According to these measurements the cross section amounts to $\sim 10^{-15}$ cm².

The process of ionization with formation of a positive and a negative ion occurs considerably more efficiently in the case in which both colliding atoms exist in the highly excited state. Thus, according to the measurements of Ref. 81, the cross section of the process $2Na(n=20) \rightarrow Na^+ + Na^-$ amounts to $\sim 10^{-12}$ cm². Such an experimental fact is rather unexpected, since an energy above 5 eV is released by the stated process, while this type of strongly

exothermic processes is usually characterized by low cross sections.

The process of ionization of highly excited atoms in collisions with electronegative molecules, e.g., SF₆,⁸²⁻⁸⁴ is also characterized by high cross-sections (see also the studies cited there):



As was established by these studies, a weakly bound electron in the collision of a Rydberg atom with an electronegative molecule behaves like a free electron whose kinetic energy equals the mean kinetic energy of the electron in the Rydberg atom. Here the cross section for the charge transfer (3.13) is close to the electron-capture cross section of the molecule. Figure 15 shows the dependences measured in Refs. 82 and 83 of the rate constants for the charge transfer between the Rydberg atoms (Rb, Na, K, Xe) and the SF₆ molecule on the principal quantum number n of the Rydberg atom. These results are comparable with the values of the rate constant for capture of a slow electron by the SF₆ molecule.⁸⁶ Since the capture cross section for a slow electron $\sim v^{-1}$ (v is the velocity of the electron), the capture-rate constant, just like the rate constant of the charge-transfer process (3.12), does not depend on the energy over a broad range of variation of the kinetic energy of the electron.

An analogous dependence of the charge-transfer constant on n has been observed⁸⁴ for Ne. According to the measurements,⁸⁴ the rate constant of the process $Ne(ns) + SF_6 \rightarrow Ne^+ + SF_6^-$ for $10 \leq n < 72$ is practically independent of n and amounts to $\approx 2 \times 10^{-7}$ cm³/s. This conclusion somewhat contradicts the results of Refs. 82 and 83 (see Fig. 15a), according to which a sharp decline in the charge-transfer constant is observed with decreasing n , even at $n < 20$ (for Na and K).

The high efficiency of the process of ionization of Rydberg atoms in collisions with electronegative atoms and molecules opens up the possibility of creating a new type of photoresonance plasma that does not contain free electrons. Another interesting line of study of the charge-transfer process involves the high-resolution spectroscopy of the Rydberg states of atoms.⁸⁷ A method of measuring the energy of highly excited states of atoms developed on the basis of the stated process is characterized by extremely high sensitivity and low error. Along this line Ref. 84 is worthy of mention, where this method was used to measure the energy of 68 excited states, as well as the ionization energy of the ²⁰Ne atom with a limit of error of 10^{-3} cm⁻¹ heretofore unattainable.

4. PROPERTIES OF PHOTORESONANCE PLASMAS

4.1. Establishment of equilibrium in photoresonance plasmas

The set of elementary processes that we have already discussed determines the parameters of a photoresonance

TABLE VI. Rate constant for ionization with formation of positive and negative ions $Rb(nl) + Rb(5s) \rightarrow Rb^+ + Rb^-$.⁸⁰

| nl | 5d | 7s | 7p | 6d | 8s | 7d | 9s | 8d | 10s |
|----------------------------------|---------------|------------|----|--------------|----|-----------|-------|-------|-------|
| $k, 10^{-14}$ cm ³ /s | $1,4 \pm 0,6$ | 10 ± 5 | 30 | 110 ± 30 | 39 | 8 ± 3 | < 6 | < 1 | < 1 |

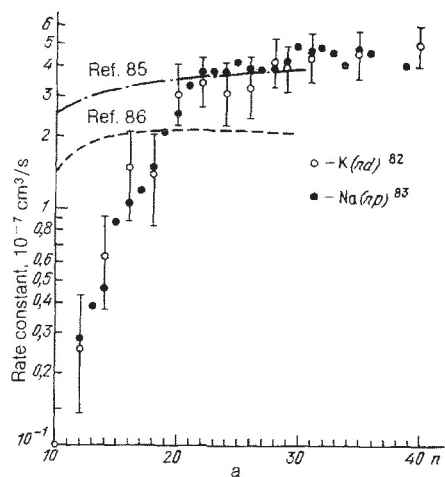
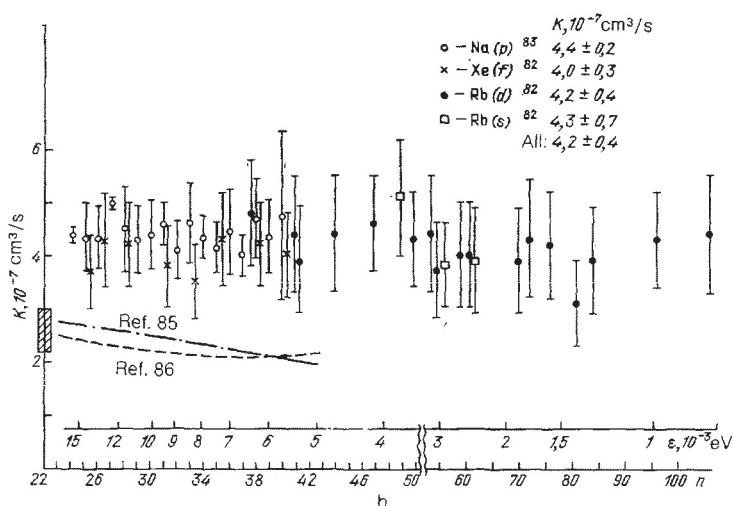


FIG. 15. Rate constant for charge transfer from a Rydberg atom to a molecule of SF_6 , as measured for different values of the principal quantum number n of Rydberg atoms of different types.^{82,83} Also presented are the results of calculating the rate constant of the process⁸⁵ $\text{Rb}(n) + \text{SF}_6 \rightarrow \text{Rb}^+ + \text{SF}_6^-$ (dotted line) and the rate constant for capture of a slow electron at an electron energy equal to the mean kinetic energy of an electron in a Rydberg atom with the given value of n ⁸⁶ (dotted line). a—Small n . b—Large n .



plasma. Below we shall make a number of estimates to get an idea of the parameters of a photoresonance plasma. Here we note that a photoresonance plasma differs substantially in its parameters from a gas-discharge plasma. The energy in a gas-discharge plasma is introduced by the action of external fields and initially is transferred to electrons, and then transferred to other degrees of freedom. In a photoresonance plasma the energy is introduced by excitation of atoms. The differing methods of excitation of gas-discharge and photoresonance plasmas have the result that, at the same electron density, the photoresonance plasma contains a larger concentration of excited atoms than the gas-discharge plasma, while the temperature of the electrons in it is appreciably lower than in the gas-discharge plasma.

To estimate the parameters of the photoresonance plasma, we shall first find out what density of excited atoms one can create by irradiating a gas or vapor with focused resonance radiation. We shall assume here that the radiation is focused on a certain region of the vapor of spherical shape, and the fundamental energy losses arise from the yield of resonance radiation from the excited atoms. In obtaining

numerical characteristics we shall restrict the treatment to the case of alkali-metal vapors. Upon allowing for the fact that the density of atoms in the $P_{3/2}$ state is twice as great as in the resonance-excited state $P_{1/2}$, we obtain the following expression on the basis of Eq. (3.5) for the total density of resonance-excited atoms:

$$N_b = \frac{AJ}{r^{5/2}}. \quad (4.1)$$

Here J is the total power of the radiation absorbed by the plasma and scattered by it, and r is the radius of the sphere; the values of the numerical coefficient A obtained from the data of Table III in the limit $T_e \ll \hbar\omega$ are presented in Table VII.⁴¹

As Table VII implies, high densities of excited states can actually be attained. For example, when $J \sim 1 \text{ W}$ and $r \sim 0.1 \text{ cm}$, we have $N_b \sim 10^{15} \text{ cm}^{-3}$, which is far higher than the densities of excited states in a gas-discharge plasma. It is precisely the density of excited states of a photoresonance plasma created by the action of the external radiation that controls the temperature and density of electrons.

In the initial stage of formation of a PRP the electron

TABLE VII. Values of the parameter A in Eq. (4.1) in the excitation of the lower resonance states of alkali-metal atoms.

| Element | Li | Na | K | Rb | Cs |
|---|-----|-----|-----|-----|-----|
| $A, 10^{12} \text{ W}^{-1} \text{ cm}^{-1/2}$ | 9,9 | 4,6 | 8,3 | 8,4 | 9,9 |

density is relatively low and the main channel of conversion of the energy of the laser radiation into plasma energy includes processes of collisions among excited atoms in (3.8) and (3.9). These processes are accompanied by formation of highly excited atoms and free electrons, whereby the density of the plasma increases. Upon exceeding a certain, rather high value of the electron density, the mechanism of energy conversion changes. Here the main channel for loss of resonance-excited atoms becomes their quenching by electron impact in (3.6), whose role proves to predominate under the condition

$$N_e \gg \frac{N_b k_p}{k_T}.$$

Here k_p is the rate constant of the faster of the processes (3.8) and (3.9). Upon substituting the characteristic values $k_i \sim 10^{-7} \text{ cm}^3/\text{s}$, $k_p \sim 10^{-10} \text{ cm}^3/\text{s}$, $N_b \sim 10^{15} \text{ cm}^{-3}$, we find that, even at $N_e \gg 10^{12} \text{ cm}^{-3}$, the energy of the resonance radiation is efficiently converted into energy of plasma electrons directly by quenching of excited atoms by electron impact. Here the electron temperature does not increase, since the energy acquired by the electrons upon quenching the resonance-excited atoms is immediately spent on ionizing atoms. Thus a quasisteady state of the plasma is established, whose parameters are determined by the density of resonance-excited atoms and the characteristics of the elementary processes in which they participate.

Generally speaking, the connection between the density of resonance-excited atoms and the parameters of the photoresonance plasma is determined by the rather complex kinetics of the radiation-collision processes in this plasma.⁴⁵ The stated kinetics must include a large number of radiation-collision transitions between excited states of the atom, diffusion of radiation and charged particles, and also ionization processes involving excited and highly excited atoms. However, the situation is substantially simplified in the limiting case of high electron density, in which all transitions between excited states of an atom are governed by its collision with electrons. Here the temperature of the electrons is relatively low, so that transitions predominate that have a change in the energy of the excited state that is small in comparison with the ionization energy.^{45,53} In this case equilibrium is established in the plasma between excited atoms existing in different states, and also between excited atoms and free electrons. Moreover, the electron density is assumed high enough that the characteristic times for ionization and recombination are much larger than the time for establishment of an equilibrium Maxwell distribution of the electrons with respect to energy.⁵¹

Let us define the equilibrium electron temperature T_0 by the following relationship:

$$\frac{N_b}{N_0} = \frac{g_b}{g_0} e^{-\Delta\varepsilon/T_0} \quad (4.2)$$

(N_0 and N_b are the densities of atoms in the ground and

excited states; g_0 and g_b are the statistical weights of these states, and $\Delta\varepsilon$ is the excitation energy of the resonance level.) Now let us formulate the equations of balance for the temperature T_e and the density of electrons N_e :

$$\begin{aligned} \frac{3}{2} N_e \frac{dT_e}{dt} = & N_e N_b k_{\text{quench}} \Delta\varepsilon - N_e N_0 k_{\text{exc}} \Delta\varepsilon + I \mathcal{K} N_e^2 \\ & - k_{\text{ion}}^{(b)} N_e N_0 (I - \Delta\varepsilon), \quad (4.3) \end{aligned}$$

$$\frac{dN_e}{dt} = -\mathcal{K} N_e^3 + k_{\text{ion}}^{(b)} N_e N_b. \quad (4.4)$$

Here k_{quench} and k_{exc} are the rate constants for quenching and excitation of the resonance levels of the atoms by electron impact, $\mathcal{K} N_e$ is the coefficient of triple recombination of electrons and ions, and k_{ion} is the rate constant of stepwise ionization of resonance-excited atoms. This notation automatically takes account of the increased rate of ionization of the atoms owing to excess concentration of the resonance-excited atoms above the equilibrium value. The equation of energy balance (4.3) takes account of the contribution, not only of processes of quenching and formation of resonance-excited atoms, but also that of ionization and recombination processes.

At relatively low values of the electron density, quenching of resonance-excited atoms is not the main channel for their loss. Therefore the temperature of the electrons in such a situation is lower than at high values of N_e in a quasi-steady-state regime. Here the contribution of the last two terms to the energy balance (4.3) is negligibly small. Upon employing the principle of detailed balancing, this enables one to represent this equation in the following form:

$$\frac{dT_e}{dt} = \frac{2}{3} N_b k_{\text{quench}} \Delta\varepsilon \left[1 - \exp\left(-\frac{\Delta\varepsilon}{T_e} + \frac{\Delta\varepsilon}{T_0}\right) \right]. \quad (4.5)$$

This implies that the characteristic time of establishment of the equilibrium temperature in a photoresonance plasma is given by the estimate

$$\frac{1}{\tau_T} \sim N_b k_{\text{quench}} \frac{\Delta\varepsilon^2}{T_0^2}. \quad (4.6)$$

In a typical situation ($N_b \sim 10^{15} \text{ cm}^{-3}$, $T_e \approx 0.3 \text{ eV}$, $k_{\text{quench}} \sim 10^{-7} \text{ cm}^3/\text{s}$, $\Delta\varepsilon \approx 3 \text{ eV}$), we have $\tau_T \sim 10^{-10} \text{ s}$, which is considerably shorter than the values of the other characteristic times for establishment of equilibrium in a photoresonance plasma. Thus, the time of establishment of the equilibrium value of the electron density can be estimated on the basis of the equation of balance (4.4), which has the following form upon allowing for the principle of detailed balancing:

$$\frac{dN_e}{dt} = \mathcal{K} N_e (N_{e0}^2 - N_e^2). \quad (4.7)$$

Here N_{e0} is the equilibrium value of the electron density as determined by the equilibrium electron temperature T_0 . The characteristic time τ_N of establishment of the equilibrium electron density is given by the estimate

$$\tau_N^{-1} \sim \mathcal{K} N_{\text{equil}}^2.$$

For example, in the case $N_e \approx 10^{16} \text{ cm}^{-3}$, $T_e \approx 0.3 \text{ eV}$, this yields $\tau_N \approx 4 \times 10^{-9} \text{ s}$, which is much larger than the time of establishment of the equilibrium electron temperature, yet much smaller than the characteristic radiative lifetimes in the photoresonance plasma.

We should note that, owing to the sharp dependence of the triple-recombination constant on the electron temperature $\mathcal{R} \sim T_e^{-9/2}$, the state of the PRP is highly critical to the magnitude of this parameter. In particular, this is indicated by the results of recent³¹ detailed experimental studies of a barium PRP formed by using laser radiation with a wavelength of 553.55 nm corresponding to the resonance transition $6s^2 \ ^1S_0 - 6s \ 6p \ ^1P_1^0$, and with a relatively low intensity (5–25 kW/cm² with a pulse duration up to 1 μ s). These experiments found a rising dependence of the occupancy of the state $6p \ ^3P_2$ of barium on the concentration of buffer gas. Here the stated dependence was sharpest in character when He was used as the buffer gas. Apparently this feature is explained by a recombination of mechanism of the occupation of this state. Adding the buffer gas reduces the electron temperature owing to processes of elastic electron-atom scattering, while the efficiency of cooling the electrons is maximal when one uses the lightest gas—helium. Thus, at a helium pressure ~ 100 Torr the characteristic time for electron cooling by elastic collisions amounts to

$$\sim \left(\frac{2m}{M} k_{\text{elast}} N_{\text{He}} \right)^{-1} \sim 10^{-7} \text{ s}$$

(Here m and M are respectively the masses of the electron and the atom; $k_{\text{elast}} \sim 10^{-8} \text{ cm}^3/\text{s}$ is the constant of elastic scattering of an electron by a helium atom). The time that is obtained is much smaller than the time of recombinative decay of the plasma for $N_e \sim 10^{14} \text{ cm}^{-3}$ and $T_e \approx 0.2\text{--}0.3 \text{ eV}$. Yet is is much larger than the time of recombinative decay of a plasma with $N_e \approx 10^{14} \text{ cm}^{-3}$ and $T_e \approx 0.03 \text{ eV}$. This implies that the intensive recombinative decay of the plasma, which leads to effective occupation of the 3P_2 state and other long-lived excited states of the barium atom, occurs in a time of the order of that of electron cooling by elastic collisions. Thus it turns out that the type and amount of the buffer gas exert a decisive influence on the efficiency of recombinative occupancy of the excited states of the atom. Primarily this pertains to the triplet states of the barium atom, which are characterized by a relatively low efficiency of collisional mixing with the singlet states that are occupied as a result of optical excitation.

The time of establishment of the equilibrium density of resonance-excited states agrees in order of magnitude with the time of exit of a resonance photon from the plasma, which is^{45,53}

$$\tau_{\text{res}} \sim \tau_0 (k_0 r)^{1/2}.$$

Here τ_0 is the radiative lifetime of the excited state, k_0 is the absorption coefficient of a photon at the center of the line, and r is the dimension of the region occupied by the plasma. For the discussed example with $r \sim 0.1 \text{ cm}$, this estimate yields $\tau_{\text{res}} \sim 10^{-6} \text{ s}$. That is, the stated time substantially exceeds the characteristic times of establishment of the electron temperature and density.

Upon taking account of the expressions written above for the exit time of the resonance radiation from the plasma, the equation of balance for the density of resonance-excited atoms N_b has the form

$$\frac{dN_b}{dt} = N_0 I \sigma_{\text{abs}} - N_b \left(\frac{1}{\tau_{\text{res}}} + I \sigma_{\text{stim}} \right). \quad (4.8)$$

Here σ_{abs} and σ_{stim} are respectively the cross section for absorption of a resonance photon by an atom and that for

stimulated emission of a resonance-excited atom, $I = \rho c$ is the flux density of the resonance radiation, and ρ is the density of resonance photons. The solution of Eq. (4.8) with the initial condition $N_b(t=0) = 0$ has the form

$$N_b = \frac{N_0 I \sigma_{\text{abs}}}{\tau_{\text{res}}^{-1} + I \sigma_{\text{stim}}} \left\{ 1 - \exp \left[-t \left(\frac{1}{\tau_{\text{res}}} + I \sigma_{\text{stim}} \right) \right] \right\}. \quad (4.9)$$

As we see, the characteristic time of establishment of the equilibrium value of the concentration of resonance-excited atoms depends on the intensity of the incident resonance radiation. When $I \ll 1/\tau_{\text{res}} \sigma_{\text{stim}}$, which corresponds to an intensity of laser radiation of the order of 10 W/cm^2 ,⁶¹ this time is close to τ_{res} . In the opposite limiting case (saturation regime), the stated time is $\sim (I \sigma_{\text{stim}})^{-1}$. At intensities exceeding 100 W/cm^2 the time of establishment of the equilibrium value of the density of resonance-excited atoms is smaller than all other characteristic times in the photoresonance plasma.

Heating of the vapor under the action of the laser radiation can cause it to disperse if this vapor exists in the form of a jet or beam. The characteristic time of dispersal τ_{disp} is $\sim r/v_{\text{th}}$, where v_{th} is the thermal velocity of the atoms. In the example we are discussing ($r \sim 0.1 \text{ cm}$) we have $\tau_{\text{disp}} \sim 10^{-5} \text{ s}$. That is, the equilibria discussed above succeed in being established even in a dispersing plasma.

The heating of the atoms and ions in a photoresonance plasma results from collisions of electrons with the atoms and ions to impart energy to the heavy particles. If we assume that this process is governed by elastic collisions of the electrons and atoms, we have an equation of balance for the mean energy $\bar{\epsilon}$ of the atoms⁵³:

$$\frac{d\bar{\epsilon}}{dt} = - \left\langle \frac{mv^2}{2} J_{\text{cr}}(f) \right\rangle = \frac{m}{M} \left(\frac{T_e}{T} - 1 \right) \langle m v^2 v_y \rangle.$$

Here m and M are the masses of the electron and the atom, T_e and T are respectively the temperatures of the electrons and the atoms, v is the velocity of the electrons, $\nu = N_e \nu \sigma^*$ is the frequency of collisions of atoms with electrons (σ^* is the diffusional cross section for scattering of an electron by an atom), and the averaging is performed over the Maxwell function of the electrons. This implies that the characteristic time for equalization of the temperatures of the electrons and the atoms is of the order of M/mv_y . In the discussed example with $N_e \sim 10^{16} \text{ cm}^{-3}$, upon assuming that $\nu \sigma^* \sim 10^{-7} \text{ cm}^3/\text{s}$, we find that $M/(mv_y) \sim 10^{-4}\text{--}10^{-5} \text{ s}$. That is, this time exceeds the other characteristic times in the photoresonance plasma. This implies that the temperatures of the atoms and electrons in the process of existence of the photoresonance plasma can differ.

The analysis that we have conducted enables us to construct a hierarchy of times in the photoresonance plasma and to elucidate the character of the establishment of equilibrium in it. Here we must bear in mind that usually experiments to create and study a PRP are performed at saturating intensities of the laser radiation ($I \gg 1/\tau_{\text{res}} \sigma_{\text{stim}}$), which can be easily attained at the present state of development of tunable lasers. In such a situation the formation of the PRP occurs at constant density of resonance-excited atoms. The initial electrons are formed by processes of collision of these atoms with one another and with unexcited atoms. With increasing

electron density, an ever greater role in the breakdown of resonance-excited atoms is played by the quenching of these atoms by electron impact. This is accompanied by an increase in the electron temperature, which continues until the process of stepwise ionization of atoms by electron impact becomes substantial. This removes from the electrons the energy that they acquire by quenching of the excited atoms. Thus a quasistationary value is established in the plasma of the electron temperature, and further formation of plasma electrons results from stepwise ionization of excited atoms by electron impact at a constant value of this parameter. The increase in electron density is accompanied by a decrease in concentration of atoms, and correspondingly, a decrease in the efficiency of absorption of the laser radiation. At a degree of ionization of the plasma of the order of unity, mechanisms of absorption owing to interaction of the radiation with collective degrees of freedom of the plasma¹⁰² become more essential than the discussed mechanism of absorption of the resonance radiation by individual atoms. In such a situation one can speak of the conversion of the PRP into a laser plasma.

Besides the collisional mechanisms of excitation and ionization of atoms discussed here, more complex mechanisms have been studied in the literature.⁴⁵ Thus, in Refs. 8 and 97, which first pointed out the important role of quenching of excited atoms by electron impact in the mechanism of converting the energy of resonance radiation into the energy of plasma electrons, processes of multiphoton absorption of laser radiation by atoms were studied as the main mechanism of ionization of atoms, rather than stepwise ionization. However, this mechanism of ionization leads to an unwarrantedly high value of the temperature of the electrons $T_e \gtrsim 1$ eV in a PRP with a high degree of ionization where, according to the results of numerous measurements,^{26-36,89} the magnitude of T_e is $\approx 0.3-0.5$ eV. Another interesting mechanism of ionization of a gas in a field of resonance radiation has been studied in Refs. 99 and 100, where the process of absorption of the energy of the electromagnetic field by electrons interacting with atoms having a resonance level is adduced as the fundamental process responsible for the heating of the electrons in the field of resonance laser radiation. By starting with the quantum kinetic equation, the authors were able to obtain the experimentally observed³¹ dependence of the rate of ionization of Ba atoms on the detuning of the frequency of the laser radiation with respect to the energy of the resonance transition. Moreover, this dependence differs little from the corresponding dependence obtained under the assumption that ionization mechanisms involving processes of multiphoton absorption play the decisive role.⁹⁷ In this regard we should note that, with the PRP parameters used in the existing experiments, electron-atom collision processes lead to formation of a PRP in times small in comparison with those measured. Therefore, for analyzing the real situation, there is no need to seek exotic mechanisms of ionization in the system. The mechanisms presented above rather fully describe the formation and establishment of equilibrium in a PRP.

4.2. Nonideal photoresonance plasmas

Since high electron densities are attained in a photoresonance plasma, while the electron temperatures are consid-

erably lower than in a gas-discharge plasma, it is easier to violate the condition of ideality of the plasma in a photoresonance plasma.

Let us analyze a photoresonance plasma from this standpoint. We shall characterize the degree of nonideality of the plasma by the plasma parameter⁸⁵

$$\Gamma = \frac{e^2}{r_D T_e} \quad (4.10)$$

This amounts to the ratio of the potential energy at the point of occurrence of a charge to the characteristic kinetic energy of the charged particles (r_D is the Debye-Hückel radius). In analyzing the plasma parameter we shall assume for simplicity that the temperatures of the ions and the electrons are the same. Here the higher the value of the parameter Γ is, the more strongly the ideality of the plasma breaks down.

Upon substituting into Eq. (4.10) the known equation for the Debye-Hückel radius and using the equilibrium formula of Saha for the electron density N_e , according to which

$$N_e = \left(\frac{N^2}{4} + Nn \right)^{1/2} - \frac{N}{2}, \quad n = \left(\frac{mT_e}{2\pi\hbar^2} \right)^{3/2} e^{-J/T_e},$$

we can determine the maximum value of the parameter Γ that is attained in the equilibrium plasma. This value and the parameters of the equilibrium plasma corresponding to it are shown in Table VIII (the lower number in each cell). In a PRP in which the equilibrium relationship of Saha relates the electron density to the occupancy of the resonance state we have

$$N_e = \frac{nG}{2} \left[\left(\frac{4N}{nG} + 1 \right)^{1/2} - 1 \right]. \quad (4.11)$$

Here we have used the symbols:

$$n = \left(\frac{mT_e}{2\pi\hbar^2} \right)^{3/2} \exp \left(-\frac{J - \hbar\omega}{T_e} \right), \quad G = \frac{2g_1}{g_0 + g_b},$$

while the occupancies of the ground and resonance-excited states are usually associated by the saturation relationship $N_0/g_0 = N_i/g_b$, which is valid even at relatively low intensities of resonance radiation ($\gtrsim 10^3$ W/cm³). The magnitude of the electron density at the same temperature is somewhat higher than in an equilibrium plasma. Thus the value of the parameter Γ also proves to be higher. The maximum values of this parameter calculated under the stated assumptions for a PRP are presented in the upper row of each of the cells of Table VIII.⁷⁾

As the data of Table VIII imply, breakdown of ideality of a photoresonance plasma is observed at attainable values of the parameters. We note the following circumstance that allows one to control this parameter. In the absence of an external agent the breakdown of ideality of a plasma accelerates its recombination, which reduces the density of electrons and increases their temperature, i.e., decreases the plasma parameter Γ . In a photoresonance plasma we control the density of resonance-excited atoms under the action of external radiation, and this creates a certain electron temperature and density in the plasma. Thus the plasma parameter is also controlled. Thus, at high enough values of the intensity of resonance radiation (saturation regime) the occupancies of the ground and resonance-excited states are practically equaled out. This can be treated as an effective lowering of the ionization potential of the atom by an amount equal to the excitation potential of the resonance state. This leads to a substantial lowering of the value of Γ as

TABLE VIII. Comparison of the parameters of a photoresonance and an equilibrium plasma for which the value of the plasma parameter Γ_i is maximal. The upper number in each cell corresponds to the PRP, and the lower to the equilibrium plasma.^{10,5}

| | N_e, cm^{-3} | | | | | |
|-----|-----------------------|----------------------|----------------------|----------------------|----------------------|----------------------|
| | 10^{14} | 10^{15} | 10^{16} | 10^{17} | 10^{18} | |
| Li: | Γ | 0,0165 | 0,041 | 0,096 | 0,22 | 0,46 |
| | T_e, eV | 0,011 | 0,027 | 0,066 | 0,155 | 0,35 |
| | N_e, cm^{-3} | 7,4·10 ¹³ | 6,9·10 ¹⁴ | 6,3·10 ¹⁵ | 5,5·10 ¹⁶ | 4,3·10 ¹⁷ |
| | | 7,7·10 ¹³ | 7,4·10 ¹⁴ | 6,9·10 ¹⁵ | 6,2·10 ¹⁶ | 5,3·10 ¹⁷ |
| | | | | | | |
| Na: | Γ | 0,020 | 0,050 | 0,12 | 0,26 | 0,56 |
| | T_e, eV | 0,011 | 0,029 | 0,070 | 0,16 | 0,37 |
| | N_e, cm^{-3} | 7,4·10 ¹³ | 6,9·10 ¹⁴ | 6,2·10 ¹⁵ | 5,4·10 ¹⁶ | 4,2·10 ¹⁷ |
| | | 7,7·10 ¹³ | 7,4·10 ¹⁴ | 6,9·10 ¹⁵ | 6,2·10 ¹⁶ | 5,3·10 ¹⁷ |
| | | | | | | |
| K: | Γ | 0,024 | 0,057 | 0,13 | 0,30 | 0,64 |
| | T_e, eV | 0,014 | 0,036 | 0,088 | 0,21 | 0,46 |
| | N_e, cm^{-3} | 7,4·10 ¹³ | 6,8·10 ¹⁴ | 6,2·10 ¹⁵ | 5,3·10 ¹⁶ | 4,1·10 ¹⁷ |
| | | 7,7·10 ¹³ | 7,3·10 ¹⁴ | 6,8·10 ¹⁵ | 6,1·10 ¹⁶ | 5,2·10 ¹⁷ |
| | | | | | | |
| Rb: | Γ | 0,025 | 0,061 | 0,14 | 0,32 | 0,68 |
| | T_e, eV | 0,015 | 0,038 | 0,092 | 0,22 | 0,48 |
| | N_e, cm^{-3} | 7,3·10 ¹³ | 6,8·10 ¹⁴ | 6,2·10 ¹⁵ | 5,2·10 ¹⁶ | 4,0·10 ¹⁷ |
| | | 7,7·10 ¹³ | 7,3·10 ¹⁴ | 6,8·10 ¹⁵ | 6,1·10 ¹⁶ | 5,2·10 ¹⁷ |
| | | | | | | |
| Cs: | Γ | 0,027 | 0,066 | 0,16 | 0,35 | 0,73 |
| | T_e, eV | 0,017 | 0,042 | 0,10 | 0,24 | 0,52 |
| | N_e, cm^{-3} | 7,3·10 ¹³ | 6,8·10 ¹⁴ | 6,1·10 ¹⁵ | 5,2·10 ¹⁶ | 4,0·10 ¹⁷ |
| | | 7,7·10 ¹³ | 7,3·10 ¹⁴ | 6,8·10 ¹⁵ | 6,1·10 ¹⁶ | 5,1·10 ¹⁷ |
| | | | | | | |

compared with the estimate made above. The values of Γ calculated for a saturation regime are shown in the bottom row to Table VIII. As we see by comparing the presented data, the illumination of an alkali-metal vapor with resonance radiation of strong enough intensity facilitates the conditions for obtaining a nonideal plasma.

Experimentally a supercooled, dense photoresonance plasma of sodium with a nonideality parameter $\Gamma \sim 1$ has been created.⁸⁹ A dye laser was used as the source of resonance radiation in this study. Its radiation at $\lambda = 589.0$ or 589.6 nm was amplified in three amplifying stages. The resulting output energy of resonance radiation reached 50 mJ with a pulse duration of 25 ns, peak power of 2 MW, and angular divergence of 2 milliradian. A laser beam with a transverse cross section of $\sim 3 \text{ mm}^2$, which corresponds to an intensity of incident radiation of $\approx 6 \times 10^7 \text{ W cm}^{-2}$, was directed into a cell filled with Na vapor in which a constant temperature was maintained. The parameters of the photoresonance plasma formed here were determined by analyzing the radiation emitted perpendicular to the direction of propagation of the laser beam. Information on the density of charged particles in the photoresonance plasma was reconstructed by processing the results of measurements of the width and line shift of a large number of the optical transitions of the Na atom. Here the results of the classical theory of broadening of spectral lines in a plasma were used.⁹⁰ The temperature of the electrons was estimated, on the one hand, on the basis of an estimate of the occupancies of the excited states of the atom under the assumption of local thermody-

amic equilibrium among these states. On the other hand, the magnitude of T_e was determined from the Saha formula while using the measured values of the electron density. The values of the electron temperature estimated by the two methods differed by about 20%, which lies within the limits of error of the described experiment. The results of the measurements of the electron density and temperature at different instants of time after onset of the pulse of laser irradiation

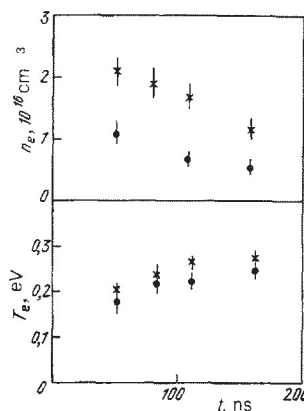


FIG. 16. Dependences of the density (a) and temperature (b) of the electrons in an Na photoresonance plasma on the time elapsed since the onset of the laser irradiation pulse. Pulse duration 25 ns, intensity of irradiation $6 \times 10^7 \text{ W/cm}^2$, cross section of the beam at the focus 3 mm . 1— $N_{\text{Na}} = 8 \times 10^{16} \text{ cm}^{-3}$, 2— $N_{\text{Na}} = 4 \times 10^{16} \text{ cm}^{-3}$.

tion are shown in Fig. 16. According to these measurements, the photoresonance plasma is characterized by the values $N_e \sim (0.5-2) \times 10^{16} \text{ cm}^{-3}$ and $T_e \sim 0.2-0.3 \text{ eV}$. This corresponds to values of the parameter $\Gamma \sim 1$. This implies that irradiation of a vapor with resonance radiation is a convenient way to create and study a weakly nonideal plasma, whose properties at present have been as yet insufficiently fully studied.

5. OPTOGALVANIC SPECTROSCOPY

5.1. The optogalvanic effect

One of the most important fields of application of the phenomenon of formation of charged particles upon irradiating a gas with resonance radiation involves the development of optogalvanic spectroscopy. This field of contemporary spectroscopy is based on detecting the fact of absorption of resonance radiation from the change in electrical characteristics of a discharge gap subject to irradiation. The mechanisms of the stated changes include sequences of elementary processes that result from formation of resonance-excited atoms, and which lead to a change in the rate of formation of charged particles. Some of these mechanisms have been discussed above in connection with the problem of formation of a PRP.

The optogalvanic effect is of interest in two applied aspects. First, it can be used to measure optical radiation of a certain frequency. The merits of this method of measurement involve the simplicity of the measuring apparatus, and also the sharp resonance character of the response of the medium to radiation of a certain frequency, which makes possible absolute calibration of the wavelength of the radiation. Another field of optogalvanic spectroscopy involves the analysis of the chemical and isotopic composition of matter. By tuning the frequency of the laser radiation to the transition of a certain atom or isotope and measuring the change in electric conductivity of the plasma caused by absorption of this radiation, the quantity of the given atoms or isotopes in the gas is established. The methods and advances of optogalvanic spectroscopy have been presented in detail in the reviews of Refs. 14, 91-93 and in the literature cited there. Here we shall analyze some mechanisms of the optogalvanic effect and study experiments in which the stated mechanisms have found the clearest manifestation.

Figure 17 shows a typical diagram of an optogalvanic experiment. The continuous radiation of the frequency-tunable laser 1 is directed through the modulator 2 into the gas-discharge tube 3. The high-frequency component of the voltage on the electrodes of the tube is taken from the ballast resistor 5 through the condenser 6; its presence is due to the

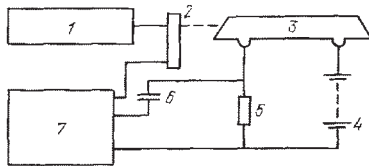


FIG. 17. Typical diagram of an optogalvanic experiment. 1—tunable laser; 2—modulator; 3—gas-discharge tube; 4—power supply; 5—ballast resistor; 6—condenser; 7—amplifier.

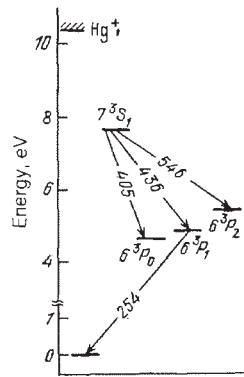


FIG. 18. Energy diagram of the states of the Hg atom participating in formation of the optogalvanic signal.⁹⁴

action on the plasma of the resonance optical radiation. This is the optogalvanic signal, which is amplified in the amplifier 7 and then recorded with appropriate apparatus. When a pulsed laser is employed, a modulator is ordinarily not used, since here the optogalvanic signal is synchronized with the pulse of laser radiation.

Both the magnitude and the sign of the optogalvanic signal are determined by the concrete mechanism of action of the resonance laser radiation on the efficiency of formation of charged particles. Let us illustrate this with the example of one of the recent experimental studies,⁹⁴ where a pulsed optogalvanic effect was observed in a low-pressure mercury discharge. Figure 18 shows an energy diagram of the states of the Hg atom that participate in forming the optogalvanic signal. A discharge tube with a current of 10 mA, diameter 19 mm, and length 50 cm, filled with mercury vapor at a density of $2.5 \times 10^{15} \text{ cm}^{-3}$ was subjected to the action of the radiation of a pulsed laser with a duration of laser pulse of 10 ms, energy $\sim 10^{-4} \text{ J}$, and wavelength 405, 436, or 546 nm, with a width of the laser line of $\sim 0.01 \text{ nm}$.

A result of the experiment being discussed was the dependence of the sign of the optogalvanic effect on the wavelength of the laser radiation. Namely, using radiation with $\lambda = 546 \text{ nm}$ decreased the conductivity of the plasma, whereas using radiation with $\lambda = 436.0 \text{ nm}$ or 405.0 nm increased this parameter. This dependence can be explained by analyzing the kinetics of ionization in a low-pressure mercury discharge. The ionization in such a discharge is stepwise in character and occurs mainly via the intermediate states $6^3P_{0,1,2}$, which are characterized by rather long lifetimes.⁹⁵ The state 7^3S_1 , which is characterized by a lifetime $\sim 10^{-8} \text{ s}$, is practically unoccupied and makes no substantial contribution to the mechanism of stepwise ionization of atoms in the discharge. Therefore the efficiency of ionization of atoms in a discharge of the type being studied is determined by the occupancies of the long-lived states $6^3P_{0,1,2}$ and the values of the stepwise-ionization constants for each of these states. Evidently the ionization constant increases with increasing energy of the long-lived state. Therefore irradiation of one of the states of the stated group, which leads to redistribution of the occupancies of these states, causes a change in the overall efficiency of formation of charged particles. Thus, when one uses radiation with $\lambda = 546 \text{ nm}$, a fraction of the excited atoms existing in the state 6^3P_2 is

converted to the state 7^3S_1 , whence it transforms by spontaneous emission to the states $6^3P_{0,1,2}$ in a ratio 15:35:50 determined by the relation between the radiative transition times. Thus, irradiation of the state 3^1P_2 leads to transition of a fraction of the atoms from this state to the lower-lying levels characterized by lower values of the rate constant for ionization. Thus the overall efficiency of ionization declines, and concomitantly also the conductivity of the gas-discharge plasma declines. The opposite situation exists when one uses radiation with $\lambda = 405$ and 436 nm, when a fraction of the atoms is converted to the higher-lying states. This is accompanied by an increase in the overall value of the ionization constant, and hence, in the conductivity of the plasma.

5.2. Laser isotope analysis

One of the most important fields of application of optogalvanic spectroscopy involves the laser isotope analysis of elements. This method of isotope analysis is incomparably simpler than the traditionally used mass-spectrometric analysis, does not require expensive vacuum and high-voltage equipment, and enables one to reduce substantially the time for measurement.

Another important advantage of the given method of isotope analysis of elements involves the high sensitivity of optogalvanic spectroscopy. To realize it, the amount of atoms that enter the discharge volume from a hollow cathode as a result of ion bombardment quite suffices.

The development of laser isotope analysis based on optogalvanic spectroscopy requires the development of accessible frequency-tunable dye lasers with a width of the laser line smaller than the isotope shift of the elements. Although this problem is still far from complete solution, already one can present a number of examples of successful use of the optogalvanic effect for isotope analysis of elements.

One of the most interesting examples of this type is Ref. 95, where the isotope composition of uranium was established by optogalvanic spectroscopy. The source of radiation in this study was a single-mode tunable dye laser (rhodamine 6G) of power up to 100 mW, and with active frequency stabilization. The laser radiation was modulated with an electrooptic modulator at the frequency of 30 kHz. The experiments employed a discharge in a hollow cathode, for which tubes made of metallic uranium were used, either of natural composition, or of uranium enriched in the isotope ^{235}U . The ballast resistance for the discharge was 2 k Ω , pressure of buffer gas (Xe) was 0.3 Torr, and the discharge current could be varied from 12 to 40 mA.

The isotope composition of uranium of natural origin was determined by irradiating the discharge tube with a laser beam with $\lambda = 591.54$ nm (transition $5^1L_0^0 \rightarrow 7^3M_7$) that was tunable in the region of absorption for the isotopes ^{238}U and ^{235}U and able to resolve the hyperfine structure of the stated transition.

Figure 19 shows the spectrum of the optogalvanic signal, which amounts to the change in the voltage across the ballast resistance under the action of the laser radiation. The partial isotope composition of natural uranium was found by processing this spectrum to be $^{235}\text{U}/^{238}\text{U} = 0.68 \pm 0.06\%$; $^{234}\text{U}/^{238}\text{U} = 0.017 \pm 0.005\%$, which agrees well with the results of mass-spectrometric measurements (0.725 and 0.0055%). The isotope composition of U enriched in the

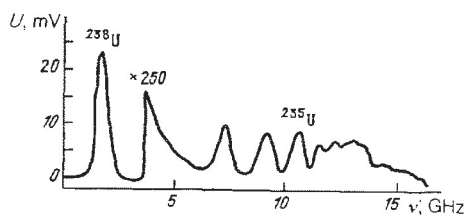


FIG. 19. Spectrum of the optogalvanic signal observed¹¹ upon irradiating U vapor of natural isotopic composition with the beam of a tunable laser ($\lambda = 591.54$ nm) in the region of the transition $5^1L_0^0 \rightarrow 7^3M_7$.

isotope ^{235}U was analyzed analogously. As an analysis of the experimental results obtained in the study showed, the described method enables one to detect admixtures of isotopes in a specimen at the level of $10^{-4}\%$ with a concentration of this admixture in the discharge of $\sim 10^6$ cm $^{-3}$.

6. CONCLUSION

As we can see from the materials presented in this review, the heightened attention paid in recent years to studies of methods of generation and of the physical properties of photoresonance plasmas is quite justified. A photoresonance plasma is an interesting physical object whose properties are determined by the multitude of elementary and kinetic processes that occur in it. Therefore the study of the properties of PRPs enriches our knowledge of the mechanisms of collisional processes that involve excited and highly excited atoms. By irradiating a gas with resonance radiation one can create a supercooled plasma with a rather high degree of ionization. In a plasma of this type one can attain values of the nonideality parameter close to unity. This makes it possible to use a PRP to study the effect of multiparticle interactions of charged particles on the electrical and thermodynamic properties of the plasma.

Studies of PRPs are not only of scientific, but also of important applied significance. Primarily this involves the realization and application of the optogalvanic effect, the essence of which lies in the change in the electrical parameters of a plasma subjected to the action of resonance radiation. The optogalvanic effect, which enables one to detect small admixtures of elements and isotopes in a gas easily and with high sensitivity, is used also for stabilizing the frequency of tunable lasers based on solutions of organic dyes, on semiconductors, and on crystals with color centers, to study the kinetics of a nonequilibrium plasma, to study elementary processes in a plasma and in a gas, to detect radiation having a certain wavelength, etc.

The frontier of studies of photoresonance plasmas continues to expand. The authors of this review hope that their publication will foster heightened activity of studies in this field and help the broad circle of readers of the journal to draw a correct picture of this interesting physical object.

¹¹We note that the values of the rate constants (cross sections) of the process (2.4) obtained in different experimental arrangements differ among themselves over a range of 1–2 orders of magnitude. As was established by the authors of Ref. 65, who analyzed this problem in detail, the stated discrepancy is explained by the difference in the velocity distributions of the excited atoms under the differing experimental conditions.

¹²We note that, e.g., for a broadening of the $3^3S_{1/2} \rightarrow 3^3P_{1/2}$ resonance line

in sodium, this criterion has the form $10 \gg \Delta\omega \gg 5 \times 10^4 \text{ s}^{-1}$.

³³Under the real conditions of a photoresonance plasma the condition of applicability of Eq. (3.10) may not be fulfilled. However, it can be used as an estimate. The other limiting case for the process (3.9) corresponds to the situation in which the atom A^{**} exists in a Rydberg state. Here we have $K_{\text{ion}} = K_{\text{quench}}$, where K_{quench} is the rate constant of quenching of a resonance-excited atom by electron impact [see Table IV, Eq. (3.6)].

³⁴We note that the presented results are valid in the region of applicability of the impact theory of broadening of spectral lines (3.4). In the region of applicability of the quasistatic theory of broadening the presented data can serve as a good estimate.

³⁵We note that these and other conditions imposed on the parameters of a low-temperature plasma in various situations have been treated in detail in the books of Refs. 45 and 53.

³⁶The numerical estimates pertain to the characteristic parameters of a photoresonance plasma of an alkali metal.

³⁷We note that, since the calculation was performed by formulas that hold for an ideal plasma, these data are in the nature of estimates. Actually, it was assumed in the calculation that the excited states are weakly occupied, the degree of ionization of the plasma is low, and the decrease in the ionization potential of the plasma was not taken into account. Moreover, we must bear in mind that, according to the result of the estimate made here, the value $\Gamma \sim 1$ is reached under conditions in which the degree of ionization of the plasma is close to unity. This also compels us to treat the presented calculation as an estimate.

³⁸A characteristic of the rate of decay of the resonance state 6^3P , is the effective lifetime. Owing to the effect of radiation trapping, this value is 2-3 orders of magnitude greater than the intrinsic lifetime of this level ($\sim 10^{-7} \text{ s}$).

¹F. Mohler and C. Boeckner, *J. Res. Nat. Bur. Standards* **5**, 399 (1930).

²N. D. Morgulis, Yu. P. Korchevoi, and A. M. Przhonskii, *Zh. Eksp. Teor. Fiz.* **53**, 417 (1967) [*Sov. Phys. JETP* **26**, 279 (1968)].

³a) A. N. Klyucharev and N. N. Bezuglov, *Processes of Excitation and Ionization of Atoms upon Light Absorption* (in Russian), Izd-vo Leningr. un-ta, L., 1983; b) A. N. Klyucharev, *Plasma Chemistry* (in Russian), ed. B. M. Smirnov, *Energoatomizdat*, M., 1980, N. 7, p. 109.

⁴N. D. Morgulis and Yu. P. Korchevoi, *Pis'ma Zh. Eksp. Teor. Fiz.* **8**, 313 (1968) [*JETP Lett.* **8**, 192 (1968)].

⁵N. D. Morgulis and A. M. Przhonskii, *Zh. Eksp. Teor. Fiz.* **58**, 1873 (1970) [*Sov. Phys. JETP* **31**, 1005 (1970)]; *Zh. Tekh. Fiz.* **41**, 992 (1971) [*Sov. Phys. Tech. Fiz.* **16**, 780 (1971)].

⁶E. D. Lozanskii and O. B. Firsov, *Spark Physics* (in Russian), *Atomizdat*, M., 1975.

⁷Ya. B. Zel'dovich and Yu. P. Raizer, *Physics of Shock Waves and High Temperature Hydrodynamic Phenomena*, Academic Press, N. Y., 1966, 1967 [Russ. original, 2nd ed., Nauka, M., 1966].

⁸R. M. Measures, N. Drexell, and P. Cardinal, *J. Appl. Phys.* **50**, 2662 (1979).

⁹H. Tamura, K. Horioka, and K. Kazuya, *ibid.* **59**, 3722 (1986); M. Hijikawa *et al.*, *Appl. Phys. Lett.* **45**, 234 (1984).

¹⁰V. V. Lebedev, V. M. Plyasulya, B. I. Troshin, and V. P. Chebotaev, *Kvantovaya Elektron.* (Moscow) **12**, 866 (1985) [*Sov. J. Quantum Electron.* **15**, 568 (1985)].

¹¹R. L. Seliger *et al.*, *Appl. Phys. Lett.* **34**, 310 (1979).

¹²R. W. Dreyfus, *ibid.* **36**, 495 (1980); **38**, 645 (1981).

¹³A. C. Tam and W. Zapka, *Laser Focus*, March, 1982, p. 69; A. C. Tam, *Proc. Conference Laser-81*, New Orleans, December 1981; *J. Appl. Phys.* **56**, 4682 (1980).

¹⁴N. B. Zorov *et al.*, see Ref. 3b, No. 13, 131 (1987); V. N. Ochkin *et al.*, *Usp. Fiz. Nauk* **148**, 473 (1986) [*Sov. Phys. Usp.* **29**, 260 (1986)].

¹⁵V. S. Letokhov, *Nonlinear Selective Photoprocesses in Atoms and Molecules* (in Russian), *Fizmatgiz*, M., 1983.

¹⁶F. A. Butaeva and V. A. Fabrikant, *Studies in Experimental and Theoretical Physics* (in Russian), Nauka, M., 1959, p. 62.

¹⁷P. Rabinowitz, S. Jacobs, and G. Gould, *Appl. Opt.* **1**, 513 (1962); *Phys. Rev. Lett.* **7**, 415 (1961).

¹⁸A. N. Klyucharev and V. Yu. Sepman, *Opt. Spektrosk.* **34**, 425 (1973) [*Opt. Spectrosc.* (USSR) **34**, 241 (1973)].

¹⁹K. L. Tan and A. von Engel, *J. Phys. D* **1**, 258 (1968).

²⁰P. C. Johnson, M. J. Cooke, and I. E. Allen, *ibid.* **11**, 1877 (1978).

²¹P. C. Stangely and I. E. Allen, *Nature* **233**, 472 (1971).

²²V. B. Brodskii *et al.*, *Teplotiz. Vys. Temp.* **12**, 191 (1974) [*High Temp.* **12**, 162 (1974)]; V. B. Brodskii and A. T. Voronchev, *Zh. Tekh. Fiz.* **40**, 1927 (1970) [*Sov. Phys. Tech. Phys.* **15**, 1501 (1971)].

²³V. P. Lebedev and É. K. Kraulinya, *Uch. Zap. Latv. Un-ta* **232**, 51 (1975).

²⁴T. B. Lucatorto and T. J. McIlrath, *Phys. Rev. Lett.* **37**, 428 (1976).

²⁵T. Stasewitz, *Opt. Commun.* **35**, 439 (1980).

²⁶T. J. McIlrath and T. B. Lucatorto, *Phys. Rev. Lett.* **38**, 1390 (1977).

²⁷T. J. McIlrath, J. Sugar, V. Kaufman, D. Cooper, and W. T. Hill III, *J.*

Opt. Soc. Am. Ser. B **3**, 398 (1986).

²⁸C. H. Skinner, *J. Phys. B* **13**, 55 (1980).

²⁹T. B. Lucatorto and T. J. McIlrath, *Appl. Opt.* **19**, 3948 (1980).

³⁰H. A. Bachor and M. Kock, *J. Phys. B* **13**, L368 (1980); **14**, 2793 (1981).

³¹R. Kunemeyer and M. Kock, *ibid.* **16**, L607 (1983); A. Kallenbach *et al.*, *ibid.* **19**, 2645 (1986).

³²L. Jahreiss and M. C. E. Huber, *Phys. Rev. A* **28**, 3382 (1983).

³³T. B. Lucatorto *et al.*, *Phys. Rev. Lett.* **47**, 1124 (1981).

³⁴W. T. Hill III, *J. Phys. B* **19**, 359 (1986).

³⁵N. K. Zaitsev and N. Ya. Shaparev, Preprint of the L. V. Kirenski Institute of Physics, Siberian Branch of the Academy of Sciences of the USSR No. 208F, Part 2, Krasnoyarsk, 1982.

³⁶V. V. Lebedev, V. M. Plyasulya, and V. P. Chebotaev, *Laser Systems* (in Russian), Institute of Heat Physics, Siberian Branch of the Academy of Sciences of the USSR, Novosibirsk, 1982, p. 35.

³⁷M. E. Koch, K. K. Verma, and W. C. Stwalley, *J. Opt. Soc. Am.* **70**, 627 (1980).

³⁸I. M. Beterov, N. V. Fateev, and V. P. Chebotaev, *Opt. Spektrosk.* **54**, 947 (1983) [*Opt. Spectrosc.* (USSR) **54**, 563 (1983)].

³⁹A. De Jong and F. van der Valk, *J. Phys. B* **12**, L561 (1979).

⁴⁰R. W. Dreyfus, *Appl. Phys. Lett.* **36**, 495 (1980).

⁴¹A. N. Zherichin *et al.*, *Appl. Phys. Ser. B* **30**, 47 (1983).

⁴²M. L. Muchnik *et al.*, *Kvantovaya Elektron.* (Moscow) **10**, 2331 (1983) [*Sov. J. Quantum Electron.* **13**, 1515 (1983)]; M. L. Muchnik, *Pis'ma Zh. Tekh. Fiz.* **9**, 1291 (1983) [*Sov. Tech. Phys. Lett.* **9**, 553 (1983)].

⁴³I. M. Beterov, V. N. Ischenko, S. A. Kochubey, and V. L. Kurochkin, *Opt. Commun.* **59**, 100 (1985).

⁴⁴M. V. Ammosov, F. A. Il'kov, and Ch. K. Mukhtarov, *Interaction of Charges in the Focal Volume in the Nonlinear Ionization of a Gas with Laser Radiation*, Preprint of the IOFAN SSSR No. 79, Moscow, 1985.

⁴⁵L. M. Biberman, V. S. Vorob'ev, and I. T. Yakubov, *Kinetics of Non-equilibrium Low-Temperature Plasmas*, Consultants Bureau, N. Y., 1987 [Russ. original, Nauka, M., 1982].

⁴⁶Yu. A. Vdovin and V. M. Galitskii, *Zh. Eksp. Teor. Fiz.* **52**, 1345 (1967) [*Sov. Phys. JETP* **25**, 894 (1967)].

⁴⁷Yu. A. Vdovin *et al.*, in: *Problems of the Theory of Atomic Collisions* (in Russian), ed. Yu. A. Vdovin, *Atomizdat*, M., 1980, p. 50.

⁴⁸Yu. A. Vdovin and N. A. Dobrodeev, *Zh. Eksp. Teor. Fiz.* **55**, 1047 (1968) [*Sov. Phys. JETP* **28**, 544 (1969)].

⁴⁹B. M. Smirnov, *Asymptotic Methods in the Theory of Atomic Collisions* (in Russian), *Atomizdat*, M., 1973, p. 246.

⁵⁰A. A. Radtsig and B. M. Smirnov, *Parameters of Atoms and Atomic Ions. Handbook* (in Russian), *Energoatomizdat*, M., 1986 [Engl. updated version of earlier 1980 edition: *Reference Data on Atoms, Molecules, and Ions*, Springer-Verlag, Berlin, 1985].

⁵¹I. I. Sobel'man, *Introduction to the Theory of Atomic Spectra*, Pergamon Press, Oxford, 1973 [Russ. original, *Fizmatgiz*, M., 1973 and Nauka, M., 1977].

⁵²V. P. Kraïnov and B. M. Smirnov, *Radiative Processes in Atomic Physics* (in Russian), *Vysshaya shkola*, M., 1982.

⁵³B. M. Smirnov, *Physics of Weakly Ionized Gases*, Mir, M., 1981 [Russ. original, Nauka, M., 1978].

⁵⁴B. M. Smirnov, *Excited Atoms* (in Russian), *Energoizdat*, M., 1982.

⁵⁵A. V. Eletskaïi and B. M. Smirnov, *Zh. Eksp. Teor. Fiz.* **84**, 1639 (1983) [*Sov. Phys. JETP* **57**, 955 (1983)].

⁵⁶B. M. Smirnov, *Excited Atoms and Molecules*, Wiley, N. Y., 1987.

⁵⁷E. E. Antonov and Yu. P. Korchevoi, *Ukr. Fiz. Zh.* **22**, 1557 (1977).

⁵⁸L. A. Vaïnshtein, I. I. Sobel'man, and E. A. Yukov, *Cross Sections for Excitation of Atoms and Ions by Electrons* (in Russian), Nauka, M., 1973.

⁵⁹I. P. Zapesochnyï, E. N. Postoi, and I. S. Aleksakhin, *Zh. Eksp. Teor. Fiz.* **68**, 1724 (1975) [*Sov. Phys. JETP* **41**, 865 (1975)].

⁶⁰B. M. Smirnov, *Dokl. Akad. Nauk SSSR* **187**, 787 (1969) [*Sov. Phys. Dokl.* **14**, 778 (1970)].

⁶¹B. M. Smirnov, *Teplotiz. Vys. Temp.* **24**, 239 (1986) [*High Temp.* **24**, 176 (1986)].

⁶²N. B. Kolokolov, see Ref. 3b, No. 12, 56 (1985).

⁶³B. M. Smirnov, *Usp. Fiz. Nauk* **133**, 569 (1981) [*Sov. Phys. Usp.* **24**, 251 (1981)].

⁶⁴N. N. Bezuglov, A. N. Klucharev, and V. A. Sheverev, *J. Phys. B* **17**, L449 (1984).

⁶⁵N. N. Bezuglov, A. N. Klyucharev, and V. A. Sheverev, *Zh. Prikl. Spektrosk.* **40**, 915 (1984) [*J. Appl. Spectrosc.* **40**, 637 (1984)].

⁶⁶A. N. Klyucharev, V. Yu. Sepman, and V. Vuïnovich, *Opt. Spektrosk.* **42**, 588 (1977) [*Opt. Spectrosc.* (USSR) **42**, 336 (1977)].

⁶⁷V. S. Kushawaha and J. J. Leventhal, *Phys. Rev. A* **22**, 2468 (1980).

⁶⁸E. L. Duman and I. P. Shmatov, *Zh. Eksp. Teor. Fiz.* **78**, 2116 (1980) [*Sov. Phys. JETP* **51**, 1061 (1980)].

⁶⁹R. Janev and A. Mihajlov, *Phys. Rev. A* **21**, 819 (1980).

- ⁷⁰J. Weiner and J. Boulmer, *J. Phys. B* **19**, 599 (1986).
- ⁷¹A. N. Klucharev, A. V. Lazarenko, and V. Vujnovič, *ibid.* **13**, 1143 (1980).
- ⁷²M. Cheret *et al.*, *ibid.* **15**, 3463 (1982).
- ⁷³J. Boulmer, R. Bonanno, and J. Weiner, *ibid.* **16**, 3015 (1983).
- ⁷⁴V. S. Kushawaha, *J. Quant. Spectrosc. Radiat. Transfer* **34**, 305 (1985); *Physica Ser. C* **132**, 295 (1985).
- ⁷⁵S. B. Zagrebin and A. V. Samson, *J. Phys. B* **18**, L217 (1985).
- ⁷⁶S. B. Zagrebin and A. V. Samson, *Pis'ma Zh. Tekh. Fiz.* **10**, 114 (1984) [*Sov. Tech. Phys. Lett.* **10**, 47 (1984)]; *Izv. Akad. Nauk Latv. SSR, Ser. Fiz.-Tekhn. Nauk*, No. 6, 118 (1985).
- ⁷⁷S. B. Zagrebin and A. V. Samson, *Pis'ma Zh. Tekh. Fiz.* **11**, 680 (1985) [*Sov. Tech. Phys. Lett.* **11**, 283 (1985)].
- ⁷⁸A. Z. Devdariani *et al.*, *ibid.* **4**, 1013 (1978) [*Sov. Tech. Phys. Lett.* **4**, 408 (1978)].
- ⁷⁹M. Cheret and L. Barbier, *Phys. Rev. A* **30**, 1132 (1984).
- ⁸⁰L. Barbier, M. T. Djerad, and M. Cheret, *ibid.* **34**, 2710 (1986).
- ⁸¹M. Ciocca *et al.*, *Phys. Rev. Lett.* **56**, 704 (1986).
- ⁸²B. G. Zollars *et al.*, *Phys. Rev. A* **32**, 3330 (1985); *J. Chem. Phys.* **84**, 5589 (1986).
- ⁸³I. M. Beterov *et al.*, *Z. Phys. Kl. D* **6**, 55 (1987); I. M. Beterov and N. V. Fateev, *Zh. Eksp. Teor. Fiz.* **93**, 31 (1987) [*Sov. Phys. JETP* **66**, 17 (1987)].
- ⁸⁴K. Harth, M. Raab, J. Ganz, A. Siegel, M.-W. Ruf, and H. Hotop, *Opt. Commun.* **54**, 343 (1985).
- ⁸⁵C. E. Klots, *Chem. Phys. Lett.* **38**, 61 (1976).
- ⁸⁶A. Chutjian and S. H. Alajajian, *Phys. Rev. A* **31**, 2885 (1985).
- ⁸⁷R. F. Stebbings and F. B. Dunning, eds., *Rydberg States of Atoms and Molecules*, Cambridge University Press, 1983 (Russ. transl., Mir, M., 1985).
- ⁸⁸V. E. Fortov and I. T. Yakubov, *Physics of Nonideal Plasmas* (in Russian) Publ. Branch of the Institute of Chemical Physics, Academy of Sciences of the USSR, Chernogolovka, Moscow Province, 1984.
- ⁸⁹O. L. Landen *et al.*, *Phys. Rev. A* **32**, 2963 (1985).
- ⁹⁰H. Griem, *Plasma Spectroscopy*, McGraw-Hill, N. Y., 1964 (Russ. transl., Atomizdat, M., 1969).
- ⁹¹P. Camus and R. B. Green, *J. Phys. (Paris)* **44**, C7-513 (1983).
- ⁹²W. B. Bridges, *J. Opt. Soc. Am.* **68**, 352 (1978).
- ⁹³J. E. M. Goldsmith and J. E. Lawler, *Contemp. Phys.* **22**, 235 (1981).
- ⁹⁴P. Van de Weijer and R. M. M. Cremers, *Opt. Commun.* **53**, 109 (1985).
- ⁹⁵P. Pianarosa, Y. Demers, and J. M. Gagne, *J. Opt. Soc. Am. Ser. B* **1**, 704 (1984).
- ⁹⁶A. Kopystynska and L. Moi, *Phys. Rep.* **92**, 135 (1982).
- ⁹⁷R. M. Measures, *J. Quant. Spectrosc. Radiat. Transfer* **10**, 107 (1970); R. M. Measures, P. L. Wizinowich, and P. G. Cardinal, *J. Appl. Phys.* **51**, 3622 (1980); R. M. Measures and P. G. Cardinal, *Phys. Rev. A* **23**, 804 (1981).
- ⁹⁸V. A. Kas'yanov and A. N. Starostin, *Zh. Eksp. Teor. Fiz.* **76**, 944 (1979) [*Sov. Phys. JETP* **49**, 476 (1979)].
- ⁹⁹V. A. Kas'yanov and A. N. Starostin, *Kvantovaya Elektron. (Moscow)* **8**, 125 (1981) [*Sov. J. Quantum Electron.* **11**, 68 (1981)].
- ¹⁰⁰V. A. Kas'yanov and A. N. Starostin, *Teplotfiz. Vys. Temp.* **23**, 609 (1985).
- ¹⁰¹N. N. Bezuglov *et al.*, see Ref. 3b, No. 13, p. 3 (1987).
- ¹⁰²C. J. Walsh and H. A. Baldis, *Phys. Rev. Lett.* **48**, 1483 (1982); W. Seka, *Opt. Commun.* **40**, 437 (1982); Villeneuve *et al.*, *Phys. Fluids* **27**, 721 (1984).
- ¹⁰³A. V. Eletskiĭ, Yu. N. Zaitsev, and S. V. Fomichev, *Zh. Eksp. Teor. Fiz.* **94**, No. 5 (1988) [*Sov. Phys. JETP* **67**, No. 5 (1988)].

Translated by M. V. King